

Large solar assisted grounds source heat pump systems

- Design based on a new low-temperature solar collector model

Master's thesis in Sustainable Energy Systems

ALEXANDER MALMBERG

MASTER'S THESIS IN SUSTAINABLE ENERGY SYSTEMS

Large solar assisted grounds source heat pump systems
- Design based on a new low-temperature solar collector model

ALEXANDER MALMBERG



Department of Architecture and Civil Engineering
Division of Building Services Engineering
CHALMERS UNIVERSITY OF TECHNOLOGY
Gothenburg, Sweden 2018

Large solar assisted grounds source heat pump systems
- Design based on a new low-temperature solar collector model
ALEXANDER MALMBERG

© ALEXANDER MALMBERG, 2018.

Supervisor: Martin Stålnacke, Energy Machines Sweden AB
Examiner: Jan-Olof Dalenbäck, Professor in Building Services Engineering,
Department of Architecture and Civil Engineering

Master's Thesis BOMX02-18-2
Department of Architecture and Civil Engineering
Division of Building Services Engineering
Chalmers University of Technology
SE-412 96 Gothenburg
Telephone +46 31 772 1000

Cover: A simplified schematic of an energy system using low-temperature solar collector together with a heat pump and borehole thermal energy storage

Typeset in L^AT_EX
Printed by Architecture and Civil Engineering
Gothenburg, Sweden 2018

Abstract

In order to reduce the climate impact, it is important to reduce the energy consumption in all sectors. A heat pump could be used to fulfill the heating and the cooling demand of a building. The disadvantage of a ground source heat pump is the relatively high investment cost. A major part of the total investment cost for such a energy system is because of the borehole thermal energy storage. When the heating and the cooling demand is not of the same size, the borehole thermal energy storage will be dimensioned so that the temperature in the storage won't drop too much after a few years. If the temperature in the storage drops it will lead to a performance drop in the heat pump.

This master's thesis examines the possibility of reducing the size of the borehole thermal energy storage by recharging the storage with a low-temperature solar collector. The cost saving for the borehole thermal energy storage is compared to the cost that the low-temperature solar collector contributes.

The research has been done on an existing building in Umeå, Sweden. First, a model of a low-temperature solar collector was built in MATLAB. The model was then validated against the solar thermal collector model in TRNSYS developed by Bengt Perers, senior researcher at Technical University of Denmark. The energy output from the low-temperature solar collector together with the energy demands and the electricity consumption of the heat pump for the investigated building were used as inputs to the model of the borehole thermal energy storage in Earth Energy Designer.

Despite the relatively large cooling demand for the examined building that could be used for charging, the results shows that it would be possible to have a smaller borehole thermal energy storage, if it was recharged with a low-temperature solar collector. If such an energy system would be built today it would be possible to lower the total investment cost of the energy system, if recharging the borehole thermal energy storage with a low-temperature solar collector.

Keywords: Solar thermal collector, Low-temperature solar collector, Ground source heat pump, Borehole thermal energy storage, Heat pump, Energy system, EnergyMachines™

Sammanfattning

För att minska klimatpåverkan är det viktigt att minska energiförbrukningen i alla sektorer. En bergvärmepump går att använda för att tillgodose värme- och kylbehoven för en byggnad. Nackdelen med bergvärme är den förhållandevis höga investeringskostnaden. En stor del av kostnaden kommer ifrån borrhållslagret. Om det inte är balans mellan värme- och kylbehovet behöver borrhållslagret dimensioneras så att inte det kyls ner för mycket under några års tid. Om temperaturen i borrhållslagret sjunker, så sjunker även värmepumpens prestanda.

Detta masterarbete undersöker möjligheten att minska borrhållslagret genom att återladda det med lågtemperatursolfångare. Kostnadsbesparingen för borrhållslagret jämförs med den kostnad som lågtemperatursolfångaren bidrar med.

Undersökningen har gjorts på en befintlig byggnad i Umeå, Sverige. Först togs en modell för en lågtemperatursolfångare fram i MATLAB. Modellen validerades mot solfångarmodellen i TRNSYS som utvecklats av Bengt Perers, forskare vid Danmarks Tekniske Universitet. Energin från lågtemperatursolfångaren tillsammans med energibehovet och elförbrukningen från värmepumpen för den undersökta byggnaden användes som indata till modellen av borrhållslagret i Earth Energy Designer.

Trots relativt stort kylbehov för den undersökta byggnaden som går att nyttja för återladdning visar resultaten att det är möjligt att ha ett mindre borrhållslager om det återladdades med lågtemperatursolfångare. Om ett sådant system skulle byggas på nytt, skulle det vara möjligt att sänka den totala investeringskostnaden för energisystemet genom att återladda borrhållslagret med lågtemperatursolfångare.

Nyckelord: Solfångare, Lågtemperatursolfångare, Bergvärme, Borrhållslager, Kylvärmepump, Energisystem, EnergyMachines™

Acknowledgements

This master's thesis has been conducted during the autumn of 2017 on behalf of Energy Machines Sweden AB. It is a part of my master's degree in Sustainable Energy Systems at Chalmers University of Technology.

First of all, I want to thank Torbjörn Sjögren and my supervisor Martin Stålnacke at Energy Machines Sweden AB who gave me the possibility to do this thesis. I also want to thank them for the support during my work.

I also would like to thank my supervisor and examiner Jan-Olof Dalenbäck at the division of Building Services Engineering at Chalmers University of Technology for the guidance.

There are some more people at Energy Machines Sweden AB I want to thank. I want to thank Viktor Hemgren and Lasse Thomsen for the technical support when creating a model of a low-temperature solar collector and a model of the borehole thermal energy storage. I also want to thank Hans-Göran Göransson who gave me the knowledge about borehole thermal energy storage.

I want to thank Bengt Perers at Technical University of Denmark for helping me create a model of low-temperature solar collector in TRNSYS to validate my MATLAB-model against.

Finally, I want to thank my fiancée, Elin Gerdin, for the support you have given me during this project.

Alexander Malmberg, Gothenburg, 2018

Contents

Terminology	1
1 Introduction	3
1.1 Background	3
1.2 Objective	3
1.3 Delimitations	4
1.4 Literature Review	4
2 Theory	7
2.1 The Basic Heat Pump	7
2.2 Borehole Thermal Energy Storage	9
2.2.1 Recharging	10
2.2.2 Dimensioning	11
2.3 Geology	13
2.3.1 Temperature	13
2.3.2 Thermal Capacity	13
2.3.3 Thermal Conductivity	13
2.3.4 Thermal Diffusivity	14
2.4 Solar Thermal Collectors	14
3 Method	17
3.1 Heat Transfer for Solar Thermal Collectors	17
3.1.1 Flat Plate Collector	18
3.1.2 Low-Temperature Solar Collector	18
3.2 Model of Low-Temperature Solar Collector	23
3.2.1 Conditions	24
3.2.2 Validation	25
3.3 Integration with EnergyMachines™ and Borehole Thermal Energy Storage	26
4 Results	29
4.1 Solar Thermal Collector	29
4.1.1 Validation	29
4.1.2 Implementation of Solar Thermal Collector in Umeå	31
4.1.3 Sensitivity Analysis	35
4.1.4 Cost of Low-Temperature Solar Collector	37
4.2 Potential Savings in Investment Cost with Low-Temperature Solar Collector	39
5 Discussion	43
5.1 Model of Low-Temperature Solar Collector	43
5.2 Integration with EnergyMachines™ and Borehole Thermal Energy Storage	44
6 Conclusion	47
References	49

Appendix A	MATLAB	i
Appendix B	TRNSYS	xi
Appendix C	EED	xiii

List of Figures

2.1	Figure (a) shows a schematic of a heat pump and Figure (b) shows the heat pump process in a Mollier diagram.	7
2.2	A simplified schematic of EnergyMachines™. [12]	8
2.3	Schematic of a heat pump using borehole thermal energy storage operating with heating.	9
2.4	Schematic of a heat pump using borehole thermal energy storage operating with cooling.	10
2.5	Figure (a) shows the annual solar energy per square meter in Sweden. Figure (b) shows how the energy varies depending on the angle. The graphs show the condition in Stockholm during sunny days [24].	16
3.1	A variant of low-temperature solar collector [27].	23
3.2	Inlet temperature to low-temperature solar collector.	25
3.3	How the low-temperature solar collector is integrated in the system.	27
3.4	Borehole configuration.	28
4.1	Comparison of the models with regards to power-output with weather condition for Arlanda.	29
4.2	Zoomed in view of Figure 4.1 for a week in May.	30
4.3	Comparison of the energy gain for different inlet temperatures with weather condition for Arlanda.	30
4.4	Total energy gain from a low-temperature solar collector compared with a glazed flat plate solar collector for different inlet fluid temperature. The plot also shows the contribution from radiation, convection and condensation for the low-temperature solar collector.	31
4.5	The total power-output from a low-temperature solar collector in Umeå.	32
4.6	The power contribution from solar radiation for a low-temperature solar collector.	32
4.7	The power contribution from condensation for a low-temperature solar collector	33
4.8	The power contribution from convection for a low-temperature solar collector.	33
4.9	ΔT between the inlet and outlet for a low-temperature solar collector module of 12 m ²	34
4.10	Energy for different inlet temperatures with weather condition like Stockholm.	36
4.11	Energy for different inlet temperatures with weather condition like Gothenburg.	36
4.12	Required borehole length according to EED and the cost savings with a low-temperature solar collector.	40
4.13	Required borehole length according to EED and the cost savings with a low-temperature solar collector, assuming no operation of the solar collector during June, July and August.	42
4.14	Required borehole length according to EED and the cost savings with low-temperature solar collector, if more than 240 m ² solar collector is present there will be no operation of the solar collector during June, July and August.	42

List of Tables

3.1	Weather condition in Umeå, mean value for each month.	24
3.2	Yearly energy demand and consumption by the energy system.	26
3.3	Bedrock conditions in Umeå.	28
4.1	Sensitivity analysis for how the different weather parameters affect the total energy gain and the contribution from radiation, convection and condensation.	35
4.2	Mean values for the different weather parameters that affect the solar collector.	36
4.3	Investment cost for a low-temperature solar thermal collector.	38
4.4	Energy output every month from a low-temperature solar collector.	39
4.5	Required borehole length according to EED and the cost savings with a low-temperature solar collector.	40
4.6	Required borehole length according to EED and the cost savings with a low-temperature solar collector, no operation of the solar collector during June, July and August.	41

Terminology

A	Area [m ²]
a ₁	Linear heat loss coefficient
a ₂	Quadratic heat loss coefficient
ATES	Aquifer Thermal Energy Storage
BTES	Borehole Thermal Energy Storage
c _p	Specific heat capacity [J/kgK]
COP	Coefficient Of Performance
D	Diameter [m]
EED	Earth Energy Designer
g	Mass flow due to condensation[kg/s]
G	Irradiation [W/m ²]
h	Heat transfer coefficient [W/m ²] or specific enthalpy [J/kg]
Isobaric process	Constant pressure
Isenthalpic process	Constant enthalpy
Isentropic process	Constant entropy
k	Thermal conductivity [W/mK]
L	Length [m]
m	Mass [kg]
ṁ	Mass flow [kg/s]
Mollier diagram	Enthalpy–entropy chart
Nu	Nusselt number
P	Power [W]
p	Pressure [Pa]
PE	Polythene
Pr	Prandtl number
PVC	Polyvinyl chloride
q	Specific heat [J/kg] or heat flux [W/m ²]
Q	Heat or Energy [J, W or Wh]
r	Radius [m]
Re	Reynolds number
rw	Energy of phase change [kJ/kg]

T	Temperature [K or °C]
\dot{v}	Volume flow [m^3/s]
V	Volume [m^3]
w	Wind speed [m/s]
x	Humidity ratio (kg water vapour per kg of dry air) [kg/kg]

Greek Letters

α	Absorptivity
ε	Specific work [J/kg] or Emissivity
η	Efficiency
λ	Thermal conductivity [W/mK]
μ	Viscosity [kg/s]
ν	Kinematic viscosity [m^2/s] or Humidity density [kg/m^3]
ρ	Density [kg/m^3]
σ	Stefan-Boltzmann constant [$\text{W}/\text{m}^2\text{K}^4$]
τ	Transmissivity

1 Introduction

This chapter presents the objectives of the thesis. It also describes the background of the thesis and delimitations that have been made.

1.1 Background

To fulfill the energy requirements for buildings in Sweden an efficient way is to use a ground source heat pump. At the moment industries want a better knowledge about the dynamics of a heat energy storage in the ground when combining the storage with a low-temperature solar collector for recharging the storage.

BTES (Borehole Thermal Energy Storage) and ATES (Aquifer Thermal Energy Storage) are the two most used techniques for heat energy storage in the ground [1, 2]. BTES is a closed-loop system, unlike ATES that is an open-loop system that uses an aquifer.

The master's thesis is done on behalf of Energy Machines Sweden AB. Energy Machines Sweden AB develops energy efficient solutions for heating, cooling and ventilation. For ventilation purpose they have developed an air handling unit called ClimateMachines™. For heating and cooling purpose they use EnergyMachines™. EnergyMachines™ is an integrated energy system consisting of two heat pumps which uses a sub-cooling technique. The system supplies properties with heating, cooling and tap water. To control their systems they use their own developed SCADA-system called ControlMachines™. SCADA is an abbreviation of supervisory control and data acquisition.

1.2 Objective

The main aim of this thesis is to dimension an integrated energy system where an EnergyMachines™ is connected to a borehole thermal energy storage together with a solar thermal collector. The thesis aims to answer the following questions.

How should the heat from the solar thermal collector be used? Should it be stored in the borehole thermal energy storage or should it be used directly in the evaporator?

How big invest would a recharging system with solar thermal collector be and how will it affect the price per kWh heat?

1.3 Delimitations

This project focuses only on Borehole Thermal Energy Storage and not Aquifer Thermal Energy Storage. For recharging the thermal energy storage, a solar thermal collector is examined in this thesis. The focus is on low-temperature solar thermal collectors. The study is made for a system with Swedish weather conditions.

1.4 Literature Review

A literature review is done to see the results from previous researches that has been done in this subject. The three most relevant researches made will be presented in this chapter together with some projects that has been built in Sweden.

In 2009 Elisabeth Kjellsson did a doctoral thesis that was about solar collectors combined with ground source heat pumps in dwellings [3]. She analyzed different system containing of solar collectors and ground source heat pumps in TRNSYS. According to her research the optimal design was to use the solar collectors for heating the domestic hot water during the summer and for recharging the energy storage during the winter. There are two important outcomes from here research. The first one is that the solution with a solar assisted ground source heat pump has it biggest advantage at existing systems were the storage is undersized, especially if the borehole length for each individual borehole is short. The second important outcome from her research is that solar collectors gives a possibility to have shorter distance between the boreholes [3].

At the 70th Conference of the ATI Engineering Association in 2015, Giuseppe Emmi et al. published there work about solar assisted ground source heat pump in cold climates [4]. The research was done on a residential building with 12 flats. The buildings energy demand is dominated by the heating demand, so the scenario in the research is simulated to have only a heat extraction from the storage. The results show that the total borehole length can be reduced when the heat pump is assisted with solar collectors [4].

In 2013 Karolis Januševičius and Giedrė Streckienė presented their work about the performance of a solar assisted ground source heat pump in the Baltic countries [5]. Their results shows that the combined system performs better than only having a ground source heat pump. The heat pump will have a more stable performance over the years and the running time for the heat pump each year is reduced with the combined system [5].

In Sweden there is a couple of existing buildings that use a solar assisted ground source heat pump. Energiförbättring Väst AB is a company in Western Sweden that has been involved in two residential projects (BRF Vårlöken and BRF Jättens Gölme) where they have installed a ground source heat pump that is assisted with hybrid solar collectors [6]. BRF Vårlöken was finished in 2013 and it is being evaluated by SP technical research institute of Sweden [7]. BRF Jättens Gölme is the biggest system in Europe of a ground source heat pump assisted by hybrid solar collectors. There are 400m² solar collectors and 270 kW ground source heat pump. The borehole thermal energy storage is designed with 28 boreholes [6, 8]. There are also a residential building in Gothenburg called Pennygängen by Stena Fastigheter that have an energy system using a ground source heat pump assisted by solar collectors. Their system is designed by Nexion [8, 9].

In 2016 was the new building for the Fredrika Bremer high school in Haninge ready. The energy system for the building was done by Norconsult. They used a system called Active Solar Energy Storage. The building is 9500m² and to fulfill the energy demand they installed 1050m² of solar collector and having an energy storage which covers an area of 6000m² below the building. The energy system is sized to be able to cover the total heating demand and having district heating as back-up [8, 10].

2 Theory

The theory chapter explains the basics for a heat pump and how the system from Energy Machines Sweden AB differ. It will also include the principle for borehole thermal energy storage and solar thermal collectors.

2.1 The Basic Heat Pump

The idea with a heat pump is to move thermal energy from a heat source with low temperature and deliver heat at a higher temperature. To be able to do that, work (ϵ) has to be added through a compressor. The other stages in the processes are condensation, expansion and evaporation [11]. A schematic of a heat pump can be seen in Figure 2.1a, and how the different stages occur in a Mollier diagram can be seen in Figure 2.1b. Between point one and two, the refrigerant has a low pressure and when it is fed with low value heat (q_2) it evaporates. After the evaporation the refrigerant will be compressed. The compression is often assumed to be isentropic. At this stage the work is added to raise the pressure and in turn raise the temperature. After the compression the refrigerant is condensed. The condensation is often assumed to be isobaric. While the refrigerant condenses it emits thermal energy (q_1) which is, for example, used for heating the radiator circuit or hot water circuit. After the condenser the refrigerant is going through an expansion valve. The expansion is assumed to be isenthalpic. The refrigerant is now back at the same low pressure as in the beginning and the process starts over [11].

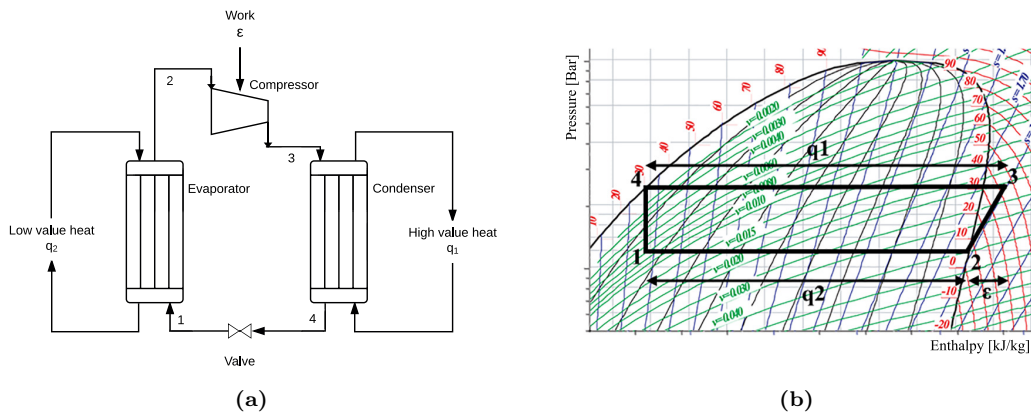


Figure 2.1: Figure (a) shows a schematic of a heat pump and Figure (b) shows the heat pump process in a Mollier diagram.

EnergyMachines™ is a heat pump system with one main heat pump (*EMA*) that delivers heat to the heating system and a second heat pump (*EMB*) that delivers heat to the domestic hot water or used to achieve a higher COP. The refrigerant in the main heat pump is sub-cooled and the rejected heat is used in the evaporator in the second heat pump and also to preheat the domestic hot water (*EMHW*) [12]. Figure 2.2 shows a simplified schematic of an energy system with EnergyMachines™. This solution enables the system to work with a higher COP-factor than a conventional heat pump [13].

When there is no need for heating the domestic hot water the second heat pump could heat the heating system as well. Since the second heat pump work with a higher COP-factor due to the higher temperature in the evaporator the overall COP-factor will increase during this operation [13].

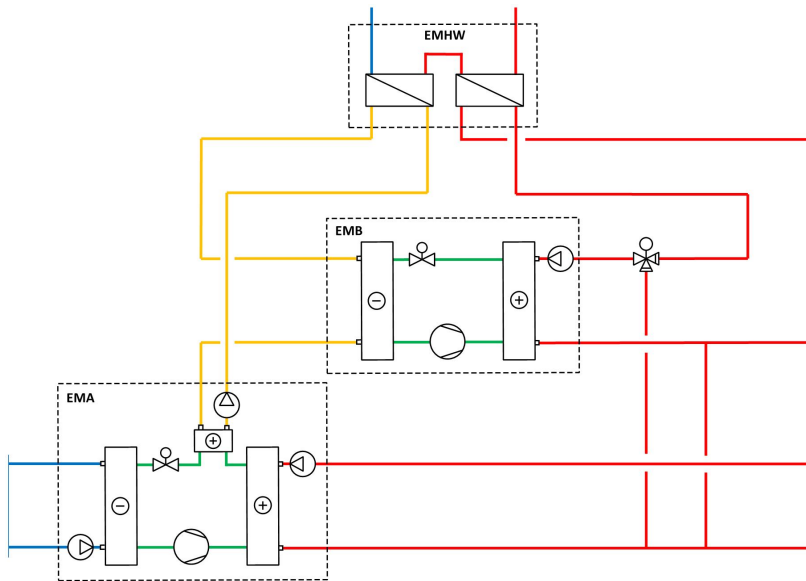


Figure 2.2: A simplified schematic of EnergyMachines™. [12]

2.2 Borehole Thermal Energy Storage

The bedrock can be used to store energy in the form of heat. The heat stored in the bedrock can be used together with a heat pump to heat buildings. By drilling holes in the ground and installing collector tubes filled with a liquid, the heat in the bedrock will be transferred from the bedrock to the liquid through conduction and convection. The collector tubes operate as a heat exchanger. The borehole depths usually vary between 100 to 300 meters and their diameter is often 115 mm, but can vary between 115 to 165 mm [14].

In a closed system the collector tubes are formed like the letter "U". A collector tube that is used often is PE DN40 PN10, where PE stands for Polythene, DN40 for a diameter of 40mm and PN denotes the maximum allowable pressure. The liquid inside the collector tube is a mixture between water and alcohol to avoid freezing. When the collector tubes are installed the wells are filled up with groundwater to improve thermal conductivity. If there are large fracture zones in the bedrock the groundwater will have a higher mass flow, which results in a better heat transfer, but this also results in a reduced ability to store energy in the bedrock. This is due to the groundwater not able to transport away heat from the rocks close to the borehole to other places in the bedrock where it will not interact with the collector tubes [15].

A system with BTES and a heat pump could be used both for heating and cooling to fulfill the need for the building. A schematic for a system operating with heating can be seen in Figure 2.3 and a system operating with cooling can be seen in Figure 2.4.

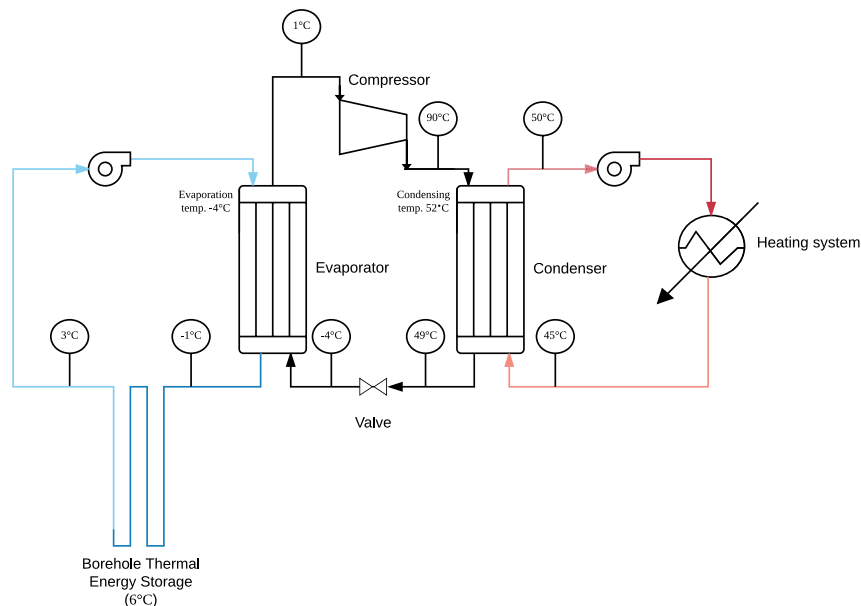


Figure 2.3: Schematic of a heat pump using borehole thermal energy storage operating with heating.

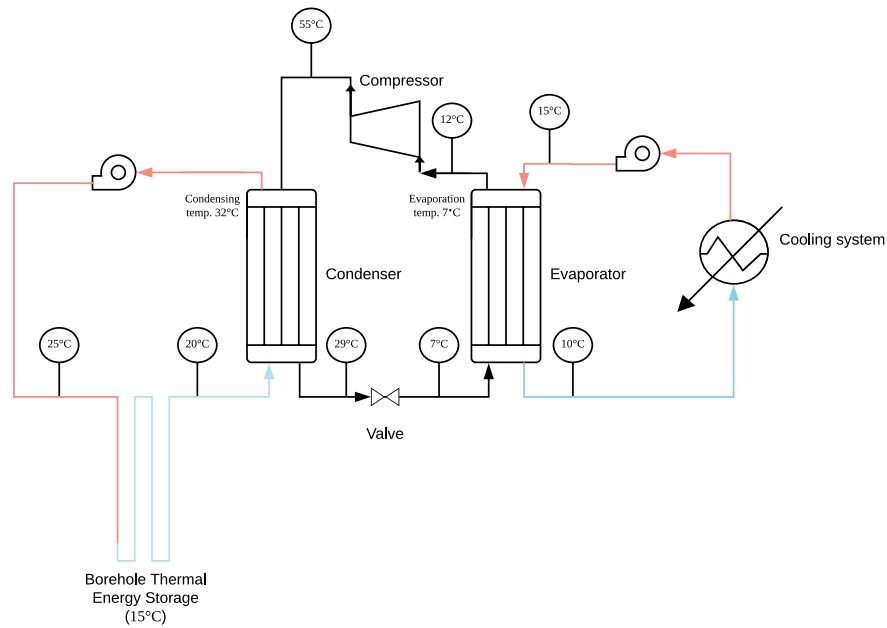


Figure 2.4: Schematic of a heat pump using borehole thermal energy storage operating with cooling.

2.2.1 Recharging

If the energy output is greater than the energy input to the bedrock, the temperature in the bedrock will drop over time. This leads to a reduced COP for the system because the temperature lift that has to be made is getting larger [15].

There is a natural recharge of the bedrock from the surroundings that depends on the temperature gradient and the thermal conductivity of the rock. In the summer the upper layer of the bedrock is recharged by the sun [14].

At high energy outages, the natural recharge is not sufficient to maintain the temperature in the bedrock. The recharging is then made when there is a surplus of heat available or when the heat energy is cheap. It is a possibility to use solar thermal collectors for recharging [15]. The recharging is limited to approximately 100 W/m [13]. With solar thermal collectors there is also a possibility to make the temperature in the bedrock higher than normal, this is good if the building has high heating demand and not a significant cooling demand.

2.2.2 Dimensioning

When dimensioning a borehole thermal energy storage it is important to have a balance in the seasonal storage. That means, to use about the same amount of energy in the form of heat as cooling over the year, otherwise the temperature in the storage will increase or decrease successively [16].

If you have a building with higher cooling demand than heating demand, an appropriate strategy may be to dimension to fulfill the cooling demand and then in the winter the heat output is limited by the storage. So in this case extra heat maybe needs to be purchased. On the other hand, if the heat demand is high compared to cooling demand, the storage should be dimension to fulfill the heating demand and then in the summer the storage can be recharged with for example solar thermal collectors [16].

A borehole thermal energy storage needs to be dimensioned both for the power and energy demand. The power output is dependent on borehole meters, the maximum output is usually 40 W/m depending on the characteristics of the bedrock. It is only the active borehole meters that are taken into account, i.e. where the collector tubes are in contact with the groundwater [13].

The energy that is possible to use depends on the bedrock volume. To calculate how big volume that is needed, the yearly energy demand, the thermal capacity of the bedrock and the temperature amplitude needs to be specified. To make a rough estimate the heat capacity is often assumed to be 0.6 kWh/m³°C and the temperature amplitude between 3-4°C. The following formula is used $V = \frac{Q}{C_p * \Delta T}$ [13].

Calculation example:

Calculate the active borehole meters and bedrock volume given the maximum power demand, yearly energy demand and the COP.

1. Calculate borehole meters

$$P_{\text{demand}} = \{\text{Maximum power demand}\} = 500[\text{kW}]$$

$$\text{COP} = \{\text{COP for this operation situation}\} = 5$$

$$P_{\text{storage}} = \{\text{Needed power output from storage}\} = \frac{P_{\text{demand}} * (\text{COP} - 1)}{\text{COP}} = 400[\text{kW}]$$

$$P_{\text{max}} = \{\text{Maximum power output per m}\} = 40[\text{W/m}]$$

$$L_{\text{b}} = \{\text{Needed borehole meters}\} = \frac{P_{\text{storage}}}{P_{\text{max}}} = \frac{400 * 1e3[\text{W}]}{40[\text{W/m}]} = \underline{10000[\text{m}]}$$

2. Calculate bedrock volume

$$Q_{\text{annual}} = \{\text{Yearly energy demand}\} = 600[\text{MWh}]$$

$$\text{COP} = \{\text{Annual COP}\} = 6$$

$$\Delta T = \{\text{Temperature amplitude}\} = 4[^\circ\text{C}]$$

$$c_{\text{p}} = \{\text{Bedrock heat capacity}\} = 0.6[\text{kWh/m}^3\text{C}]$$

$$Q_{\text{storage}} = \{\text{Yearly energy outtake from storage}\} = \frac{E_{\text{annual}} * (\text{COP} - 1)}{\text{COP}} = 500[\text{MWh}]$$

$$V = \{\text{Needed bedrock volume}\} = \frac{E_{\text{storage}}}{C_{\text{p}} * \Delta T} = \frac{500 * 1e3[\text{kWh}]}{0.6[\text{kWh/m}^3\text{C}] * 4[^\circ\text{C}]} \approx \underline{208333[\text{m}^3]}$$

Answer: Active borehole meters = 10000 [m] and bedrock volume \approx 208333 [m³]

2.3 Geology

In order to use borehole thermal energy storage some geological properties are required. Parameters that have a major impact are temperature, thermal capacity, thermal conductivity and thermal diffusivity.

2.3.1 Temperature

The maximum heat output that is possible depends on the temperature in the bedrock. The temperature of the bedrock in the south and middle of Sweden can be assumed as the same as the average annual temperature in this part of Sweden. In the north of Sweden the temperature is 1-4 degrees higher than the average annual temperature due to the insulation of snow in the winter. In 2015 the temperature in the south of Sweden was 9-10°C and in the north it was 3°C. Due to the geothermal heat flow the temperature rises by approximately 30 °C/km in the south and 15-20 °C/km in the north. The geothermal heat flow is the heat energy generated from the core of the earth. From a depth of 20 meters, the temperature is mostly affected by the geothermal heat flow and above 20 meters it's mostly affected by the climate. The surface is also affected by the radiation from the sun [14].

2.3.2 Thermal Capacity

How much energy that could be stored in the bedrock is affected by the thermal capacity. Thermal capacity is defined as the energy needed to raise the temperature of 1 kg by 1 K. This gives a measure of how much energy that could be extracted by lowering the temperature by 1 K, and also how much energy that is being stored when the temperature rises by 1 K. As an example, granite has a thermal capacity of approximately 1 kJ/kgK [14].

2.3.3 Thermal Conductivity

The two major properties for how much power output that is possible is temperature and thermal conductivity (λ or k). Thermal conductivity describes how good the bedrock conduct heat energy and it is measured in W/mK. Thermal conductivity depends on both the composition of the mineral and its physical properties, such as porosity and permeability. To decide how much power it is possible to extract for each borehole meter the thermal conductivity is a very important parameter [14].

2.3.4 Thermal Diffusivity

Thermal diffusivity describes the temperature change in the bedrock as a function of time when heat is added. It's calculated by dividing the conductivity with the capacity. The unit for thermal diffusivity is m^2/s [14].

2.4 Solar Thermal Collectors

Solar thermal collectors have a great potential for heating systems. In Sweden, the entire hot water demand in a house could be covered by a solar collector during the summer. On an annual basis, 50% of the demand could be covered by a solar thermal collector. If the solar thermal collector is combined with the heating system for the house, then about 20-30% of the total annual heat demand could be covered by the solar thermal collector [17].

The most common types of solar thermal collectors are flat plate collector, low-temperature solar collector and evacuated tube collector. Flat plate collector is the most used solar thermal collector around the world except in China, where the evacuated tube collector is most common [18]. In Sweden a flat plate collector and an evacuated tube collector costs around 2000 to 5000 SEK per square meter depending on the type [19].

Low-temperature solar collector is also called solar pool heating panel since it is mostly used to heat the water in swimming pools or other direct systems where all water circulates through the collector. Low-temperature solar collectors are very simple in their construction, consisting of only a collector tube in a synthetic material, e.g. PVC. The water inside the collector tubes is heated by the solar radiation and by the surrounding air, if the surrounding air has a higher temperature than the surface of the collector tubes. Because it is uninsulated, it has a very low efficiency when the water inside has a higher temperature than the surrounding air, and the other way around, when the temperature of the working fluid is lower than the surrounding air it has a high efficiency [20].

Evacuated tube collector consists of a glass tube around a metal tube with vacuum between for insulation, using the same principle as a thermos. The metal tube will absorb the solar radiation and becomes hot. The heat is then transported by a liquid that is flowing and cooling the inside of the metal tube [21, 17].

A flat plate collector consists of a frame that has an insulated back and a transparent front, usually glass, that lets the radiation through. Between these plates there are collector tubes of metal that absorb the radiation. As with the evacuated tube collector, a liquid flows inside the tubes that transport the heat. The insulated back and transparent front is used to minimize heat losses to the surroundings [22, 17].

To calculate how much useful energy that is produced from a flat plate collector “Hottel-Whillier-Bliss equation” could be used, see equation 2.1. The thermal efficiency of the collector is calculated with equation 2.2 [23].

$$Q_u = F_R * A * [G\tau\alpha - U_L * (T_i - T_a)] \quad (2.1)$$

$$\eta = F_R * \tau * \alpha - F_R * U_L * \frac{T_i - T_a}{G} \quad (2.2)$$

Terminology

A	Collector area [m ²]
F _R	Collector heat removal factor
G	Intensity of solar radiation [W/m ²]
T _i	Inlet fluid temperature [°C]
T _a	Ambient temperature [°C]
U _L	Collector overall heat loss coefficient [W/m ²]
Q _u	Useful energy gain [W]
η	Collector efficiency
τ	Transmission coefficient of glazing
α	Absorption coefficient of plate

The surface of the earth is reached by 750 million TWh of solar energy each year, of which Sweden's surface receives 360 000 TWh/year. The sunniest areas in the world are reached by 3400 kWh/m² each year. In Sweden, the solar radiation varies between 800kWh/m² in the north to 1000kWh/m² in the south, see Figure 2.5a. The above values are for a horizontal surface. The most optimal in Stockholm is a south-facing surface with an angle of 60° from the horizontal plane, i.e. 0° is horizontal and 90° is vertical [24].

How the solar radiation differs throughout the year for a horizontal and vertical surface in Stockholm can be seen in figure 2.5b. The closer to the equator, the less slope from the horizontal plane will be needed to receive as much energy as possible [24].

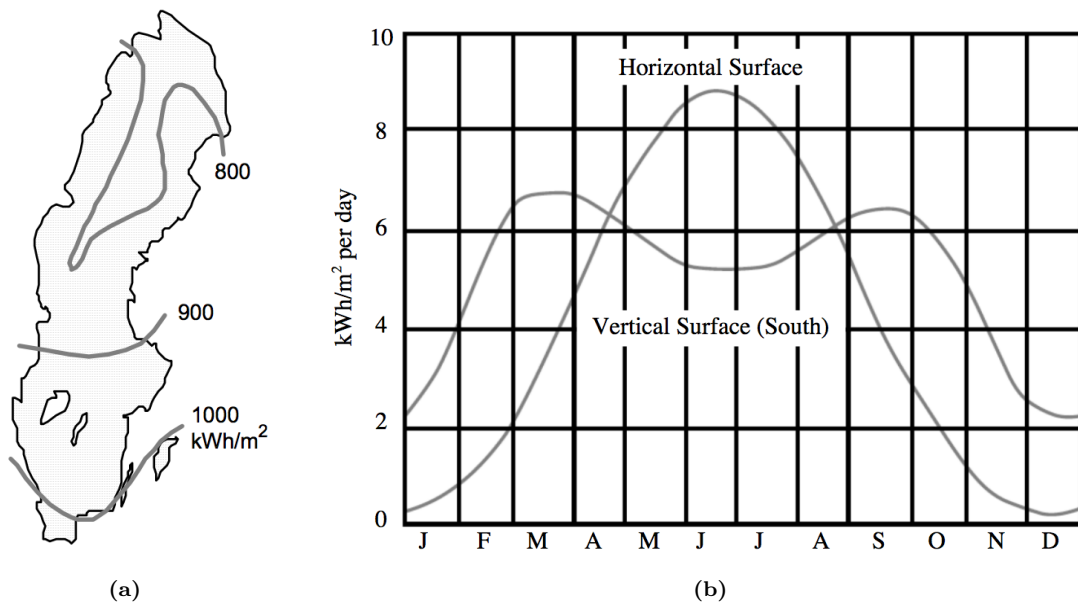


Figure 2.5: Figure (a) shows the annual solar energy per square meter in Sweden. Figure (b) shows how the energy varies depending on the angle. The graphs show the condition in Stockholm during sunny days [24].

3 Method

This chapter will first describe how the heat transfer for the different solar thermal collector is calculated. The second part is how the conditions are determined and how the model is built and validated. The last part describes how the model is integrated with EnergyMachines™ and BTES to answer the objectives.

3.1 Heat Transfer for Solar Thermal Collectors

The report will focus on two different types of solar thermal collectors, glazed flat plate collector and low-temperature solar collector. The efficiency for a glazed flat plate collector can be calculated with equation 3.1 described in chapter 3.1.1. For a low-temperature solar collector the heat transfer needs to be calculated for each type of heat transfer that occurs, due to the considerable interaction with the outdoor air. There will be a great share of heat energy from the temperature difference between the fluid and surrounding air and also in some cases condensation of the moist outdoor air. This is described in chapter 3.1.2.

3.1.1 Flat Plate Collector

The efficiency for a solar collector can be simplified into equation 3.1 [18]. The total useful energy from the solar collector is then calculated with equation 3.2. For a flat plate collector a typical value for η_0 is 0.78, a_1 is 3.2 and a_2 is 0.015 [25].

$$\eta = \eta_0 - a_1 \frac{T_m - T_a}{G} - a_2 \frac{(T_m - T_a)^2}{G} \quad (3.1)$$

$$Q = \eta * G * A \quad (3.2)$$

Terminology

A	Collector area [m ²]
a_1	Linear heat loss coefficient
a_2	Quadratic heat loss coefficient
G	Intensity of solar radiation [W/m ²]
Q	Useful energy gain [W]
T_a	Ambient temperature [°C]
T_m	Collector fluid average temperature [°C]
η_0	Optical efficiency
η	Collector efficiency

3.1.2 Low-Temperature Solar Collector

The useful energy from a low-temperature solar collector could be calculated with equation 3.3. The fluid absorbs or emits energy through three different ways.

The fluid is affected by the temperature gradient between the fluid temperature and the temperature of the surrounding air. If the temperature of the surrounding air is higher than the temperature of the fluid, there will be heat transferred from the air to the fluid. The heat transfer will be through convection between the air and the surface of the tubes and then conducted through the tube and finally internal flow convection between the inside surface and the fluid. These different types of heat transfer will be added as resistances in series and the driving force is the temperature gradient, see equation 3.4.

In some conditions the surrounding air contains so much moisture that it will condense when it is cooled down. This phase change will lead to that energy in the form of heat is transferred to the liquid.

The fluid will be affected by radiation, mainly by absorbing the solar radiance, but it will also emit heat to the surroundings by radiation. The radiation will only affect half of the outside area, assuming no interaction between the roof and the collector [11].

These equations are for one dimensional steady state conditions [11]. To calculate a large area, the collector is divided into small areas that are calculated separately. The outlet temperature of the fluid from the first small area is taken as the inlet temperature to the second small area and so on.

$$Q_{\text{tot}} = Q_{\text{convection}} + q''_{\text{condensation}} * A + \frac{q''_{\text{radiation}} * A}{2} \quad (3.3)$$

$$Q_{\text{convection}} = \frac{T_a - T_{\text{fluid}}}{\frac{1}{h_1 * 2 * \pi * r_i * L} + \frac{\ln(r_o/r_i)}{k_{\text{PVC}} * 2 * \pi * L} + \frac{1}{h_2 * 2 * \pi * r_o * L}} \quad (3.4)$$

Terminology

A	Collector tube outside area [m ²]
h ₁	Heat transfer coefficient, internal flow [W/m ² K]
h ₂	Heat transfer coefficient, convection [W/m ² K]
k _{PVC}	Thermal conductivity for PVC, = 0.19 [W/mK]
L	Length [m]
q'' _{condensation}	Heat flux from condensation [W/m ²]
q'' _{radiation}	Heat flux from radiation [W/m ²]
Q _{convection}	Energy gain from outdoor air through convection [W]
Q _{tot}	Total energy gain [W]
r _i	Inside radius of the collector tube [m]
r _o	Outside radius of the collector tube [m]
T _a	Ambient temperature [°C]
T _{fluid}	Fluid temperature [°C]

Internal flow

Inside the tube, the heat transfer is through convection due to the internal flow. The heat transfer coefficient is calculated with equation 3.9. To calculate the heat transfer coefficient, the Reynolds number and Prandtl number needs to be calculated with equations 3.5 and 3.6. If the Reynolds number is above 10000, fully developed turbulent flow can be assumed and then the Nusselt number is calculated with equation 3.8. If the Reynolds number is lower than 10000, laminar flow is assumed and the Nusselt number is constant 4.36 for a circular shaped tube with uniform heat flux, see equation 3.7 [11].

$$\text{Re}_D = \frac{\dot{v} * D}{\nu * A} \quad (3.5)$$

$$\text{Pr} = \frac{c_p * \mu}{k} \quad (3.6)$$

$$\text{Nu}_D\{\text{Laminar}\} = 4.36 \quad (3.7)$$

$$\text{Nu}_D\{\text{Turbulent}\} = 0.027 * \text{Re}_D^{4/5} * \text{Pr}^{1/3} * \left(\frac{\mu}{\mu_s}\right)^{0.14} \quad (3.8)$$

$$h_1 = \frac{\text{Nu}_D * k}{D} \quad (3.9)$$

Terminology

A	Cross-section area [m ²]
c _p	Specific heat capacity, fluid [J/kgK]
D	Inside diameter of the collector tube [m]
h ₁	Heat transfer coefficient, internal flow [W/m ² K]
k	Thermal conductivity, fluid [W/mK]
Nu	Nusselt number
Pr	Prandtl number
Re	Reynolds number
\dot{v}	Volume flow [m ³ /s]
μ	Viscosity [kg/s]
μ_s	Viscosity at surface temperature[kg/s]
ν	Kinematic viscosity [m ² /s]

Convection

The heat transfer by convection on the outside of the tubes (h_2) depends on the wind speed at the collector plane. To calculate the wind speed at the collector plane (W_{coll}) by knowing the wind speed at 10m height (w), equation 3.10 is used [26]. The heat transfer coefficient is calculated with equation 3.11[27].

$$W_{coll} = w * 0.68 - 0.5 \quad (3.10)$$

$$h_2 = 2.8 + 3 * W_{coll} \quad (3.11)$$

Radiation

The heat flux due to radiation is calculated with equation 3.12. The equation takes in account both the energy gain from radiation and the radiation losses. The solar absorptivity for PVC is 0.9 and the emissivity is 0.1 [28]. The effective sky temperature could be assumed to be -10°C [11].

$$q''_{radiation} = \alpha_s * G_s - \varepsilon * \sigma * (T_s^4 - T_{sky}^4) \quad (3.12)$$

Terminology

G_s	Solar irradiation [W/m^2]
$q''_{radiation}$	Heat flux [W/m^2]
T_s	Surface temperature [K]
T_{sky}	Effective sky temperature [K]
α_s	Surface absorptivity
ε	Emissivity
σ	Stefan-Boltzmann constant [$\text{W}/\text{m}^2\text{K}^4$]

Condensation

Depending on the outdoor air condition and the temperature of the collector tube, the outdoor air will sometimes condensate. The air will condense if the surface temperature is below the dew point for the specific moisture and temperature condition of the outdoor air. If condensation occurs, the heat flux from condensation is calculated with equation 3.15. The equation calculates the moisture flow on the surface with the help of equations 3.13, 3.14 and 3.11. The mass flow is then multiplied with the energy that the phase change entails [27].

$$\nu_{\text{air}} = \rho_{\text{air}} * x \quad (3.13)$$

$$\nu_{\text{sat}} = 10^{-5} * (485 + 34.7 * T_s + 0.945 * T_s^2 + 0.0158 * T_s^3 + 0.000281 * T_s^4) \quad (3.14)$$

$$q''_{\text{condensation}} = rw * g = rw * \frac{h_2}{\rho_{\text{air}} * c_{p,\text{air}}} * (\nu_{\text{air}} - \nu_{\text{sat}}) \quad (3.15)$$

Terminology

$c_{p,\text{air}}$	Specific heat capacity, ambient air [J/kgK]
h_2	Heat transfer coefficient, convection [W/m ²]
g	Moisture flow per m ² [kg/s]
$q''_{\text{condensation}}$	Heat flux from condensation [W/m ²]
rw	Energy of the phase change between water and steam, 2260 [kJ/kg]
T_s	Surface temperature [°C]
x	Humidity ratio (kg water vapor per kg of dry air) [kg/kg]
ρ_{air}	Density, ambient air [kg/m ³]
ν_{air}	Humidity density, ambient air [kg/m ³]
ν_{sat}	Maximum humidity density of air at the specific temperature [kg/m ³]

3.2 Model of Low-Temperature Solar Collector

To be able to calculate how much energy and power that could be generated by a low-temperature solar collector a MATLAB model was built using equations 3.1 to 3.15. The MATLAB-code is presented in Appendix A. The model calculates the energy gain and the outlet temperature for a small volume. The calculation is then iterated to get the desired size of the low-temperature solar collector, with the outlet temperature as the new inlet temperature. The low-temperature solar collector in the model is made of DN40 tubes that are put in a rectangular shape, like the collector in Figure 3.1. Each module is made of 160 m tubes that form a 2x6 m rectangular. To make a larger low-temperature solar collector, this module of 12 m² is connected in parallel. The flow trough each module is set constant to 0.4 l/s, which gives a pressure drop of 40 kPa.



Figure 3.1: A variant of low-temperature solar collector [27].

3.2.1 Conditions

To be able to do the calculation there are some conditions that needs to be specified. The outdoor condition such as temperature, relative humidity, wind speed and solar irradiation are taken as hourly values from SMHI's database [29].

In this report the low-temperature solar collector is implemented in a condition similar to Umeå. Where the solar irradiance varies between 0 and 785 [W/m^2], the air temperature between -12.6 and 26.6 [$^{\circ}\text{C}$], the relative humidity between 34 and 100 [%] and the wind speed between 0 and 17.2 [m/s]. The mean value for each month is shown in table 3.1. The model is also investigated in a condition similar Stockholm and Gothenburg to understand how the weather condition will affect the low-temperature solar collector.

Table 3.1: Weather condition in Umeå, mean value for each month.

Month	Solar irradiance [W/m^2]	Ambient temperature [$^{\circ}\text{C}$]	Relative humidity [%]	Wind speed [m/s]
January	5.4	-2.6	90.6	6.1
February	28.0	-0.5	88.3	3.9
March	94.7	0.9	84.0	4.9
April	144.4	3.3	83.4	5.1
May	219.4	6.7	75.8	4.5
June	235.3	10.7	78.5	4.1
July	207.6	14.9	80.4	3.9
August	154.2	16.6	83.8	4.9
September	77.1	12.4	89.9	3.9
October	30.4	6.3	88.3	4.8
November	8.4	3.2	91.9	6.0
December	2.8	0.9	89.6	5.4
Annual mean value	101.1	6.1	85.3	4.8

The temperature of the fluid that enters the solar collector will vary between 0.5 °C in the winter and 26.8 °C in the late summer with a mean value of 6.4 °C. How the temperature differ over the year is shown in Figure 3.2. This temperature corresponds to the temperature before the collector fluid goes to the BTES. How the collector fluid temperature in the bedrock will be affected by a low-temperature solar collector can be seen in Appendix C. The temperature difference between the case with and without a low-temperature solar collector is small so it doesn't have a major impact on the energy output from the low-temperature solar collector. Therefore the inlet temperature to the low-temperature solar collector could be assumed to be like Figure 3.2. This assumption can not be made on a smaller system or a system with a larger difference between the heating and cooling demand.

The model calculates the heat transfer on the inside with properties for water, but in reality it will be a mixture, for example between water and glycol to prevent freezing and vaporization inside the collector.

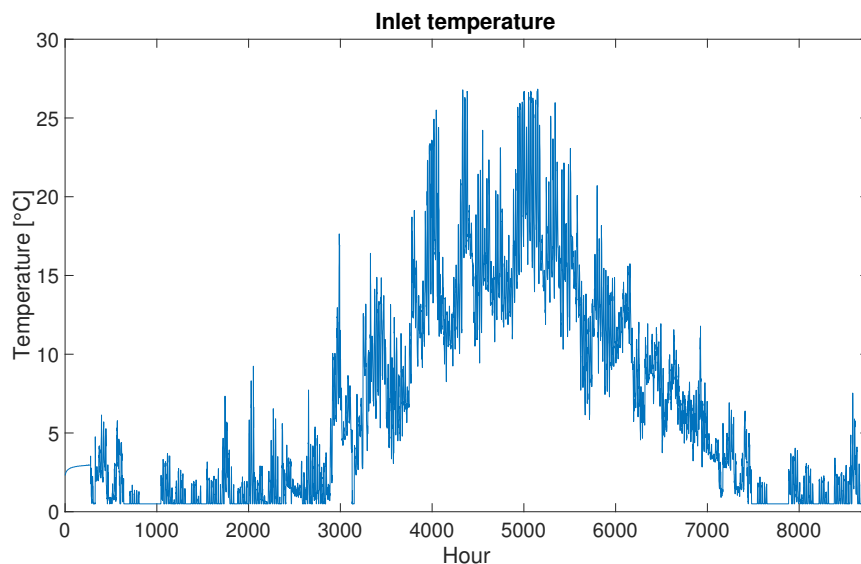


Figure 3.2: Inlet temperature to low-temperature solar collector.

3.2.2 Validation

To validate the MATLAB model, a model for an unglazed flat plate collector that works below the dew point is built in TRNSYS in cooperation with Bengt Perers, senior researcher at Technical University of Denmark. In TRNSYS there is a component called Type832. This component has been developed by Bengt Perers and works with temperatures below the dew point.

A comparison between the model in MATLAB and the model in TRNSYS is made. Both the power output during a year with a constant inlet temperature of 5 °C and the energy output during the year for different inlet temperatures is compared. The weather data stored in TRNSYS for Arlanda is used.

3.3 Integration with EnergyMachines™ and Borehole Thermal Energy Storage

To integrate the model of a low-temperature solar collector with EnergyMachines™ and BTES, data from a specific case, including an EnergyMachines™ and BTES is extracted with help of ControlMachines™. The data that are of interest is the heating and cooling demand and the energy consumed by the energy system, see table 3.2. By knowing these values it is possible to calculate how much energy that is needed to be extracted/recharged from the BTES. The energy that is extracted from the BTES is the heat demand subtracted the cooling demand and energy used by the energy system, if this value is negative it means that the BTES is being recharged.

To simulate how the BTES design will be affected when implementing a low-temperature solar collector in the system, a model in EED is created where the energy from the low-temperature solar collector aide the BTES. It is assumed that the energy from the low-temperature solar collector is possible to store in the BTES and in cases when the fluid extract energy from the BTES, the energy that needs to be extracted is the original demand subtracted with the energy from the low-temperature solar collector.

Table 3.2: Yearly energy demand and consumption by the energy system.

Month	Heating demand [kWh]	Cooling demand [kWh]	Energy consumed by the heat pump system [kWh]
January	574 192	216 584	150 928
February	639 722	160 901	196 410
March	701 067	223 274	221 381
April	712 508	274 431	218 982
May	454 357	408 771	123 960
June	272 995	501 898	115 488
July	176 816	584 243	126 484
August	252 721	536 285	125 918
September	381 266	402 849	113 556
October	588 475	344 435	163 483
November	675 391	185 554	197 579
December	692 555	194 978	221 505
Total	6 122 065	4 034 203	1 975 674

The low-temperature solar collector will be connected to the borehole thermal energy storage through a plate and frame heat exchanger, see Figure 3.3. Since there is an ethanol mixture in the borehole thermal energy storage and a glycol mixture in the low-temperature solar collector to avoid freezing and vaporization.

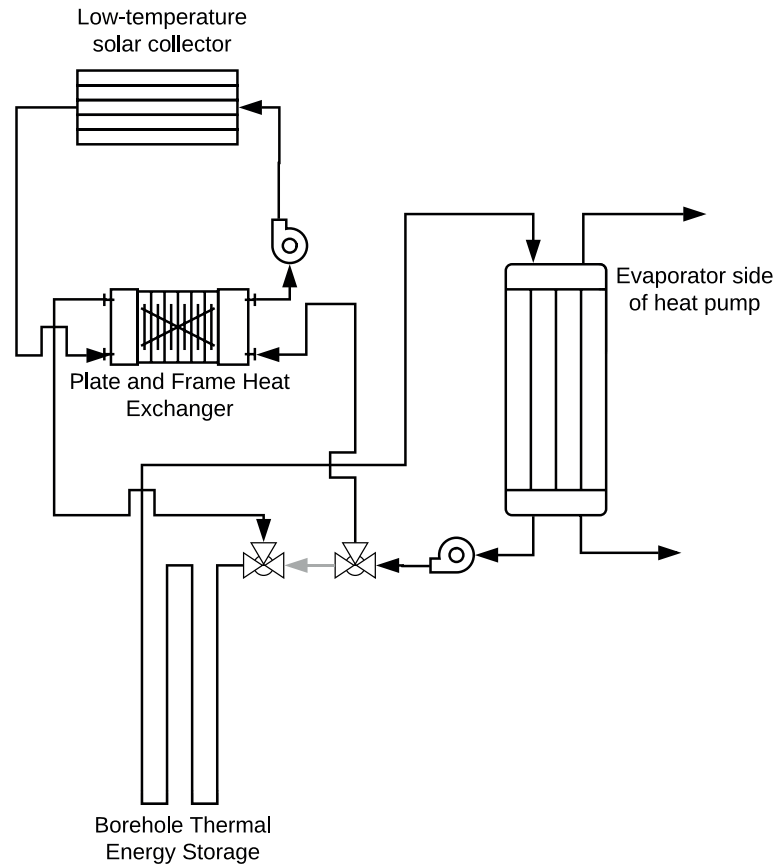


Figure 3.3: How the low-temperature solar collector is integrated in the system.

A model of the borehole thermal energy storage is made in EED. The volume flow to the storage is assumed to be 37.5 l/s and the borehole is 114.3mm with an U-pipe DN50, see Figure 3.4. The borehole is filled with water and the collector fluid is water with 15% ethanol. The bedrock parameters are taken for a condition similar to Umeå, see table 3.3.

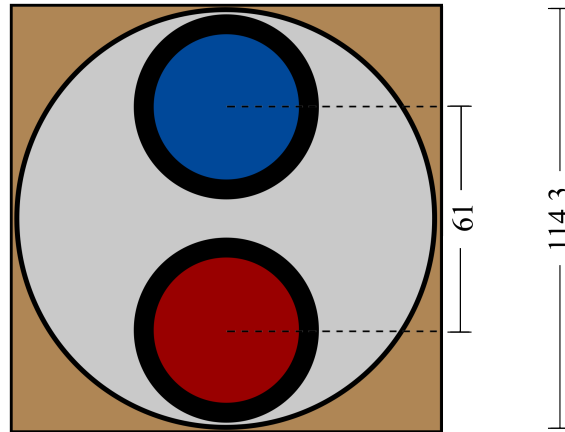


Figure 3.4: Borehole configuration.

Table 3.3: Bedrock conditions in Umeå.

Parameters	
Thermal conductivity	3.4 [W/mK]
Volumetric heat capacity	2.3 [MJ/m ³ K]
Ground surface temperature	4.5 [°C]
Geothermal heat flux	0.05 [W/m ²]

With these parameters and energy input from table 3.2, EED calculates the design that require least number of boreholes meters. The borehole design needs to keep the borehole spacing between 3 and 15 m, the borehole depth between 200 and 320m and the fluid temperature after the BTES needs to be between -2 and 25°C to be able to keep the COP in both heating and cooling mode.

The simulation is then made for several cases with different sizes of the low-temperature solar collector. Simulations are also made in cases when the low-temperature solar collector is not used in the summer. In the summer there is a surplus of heat that is already recharging the BTES. The reason to close down the low-temperature solar collector in the summer is to avoid the temperature in the BTES to get too high.

4 Results

The result chapter will present the results for the model of a low-temperature solar collector in MATLAB. The results contain the possible power and energy output and also the validation and sensitivity analysis.

The investment cost that a low-temperature solar collector brings will be present for different sizes of the collector. The results also include how the BTES is affected and how much that is possible to save in investment cost for the energy system.

4.1 Solar Thermal Collector

This chapter presents the validation of the MATLAB-model. It also shows the energy gain and power if the low-temperature solar collector would have been implemented in Umeå and a comparison with other weather conditions to see how sensitive the results are. Finally the investment cost for a low-temperature solar collector will be presented.

4.1.1 Validation

The validation is made between the MATLAB-model and a model in TRNSYS using the component called Type832v501. The power-output per square meter of the both models, using the weather data for Arlanda that are stored in TRNSYS and the inlet temperature constant 5 °C are presented in Figure 4.1. Figure 4.2 shows the results for a week in May.

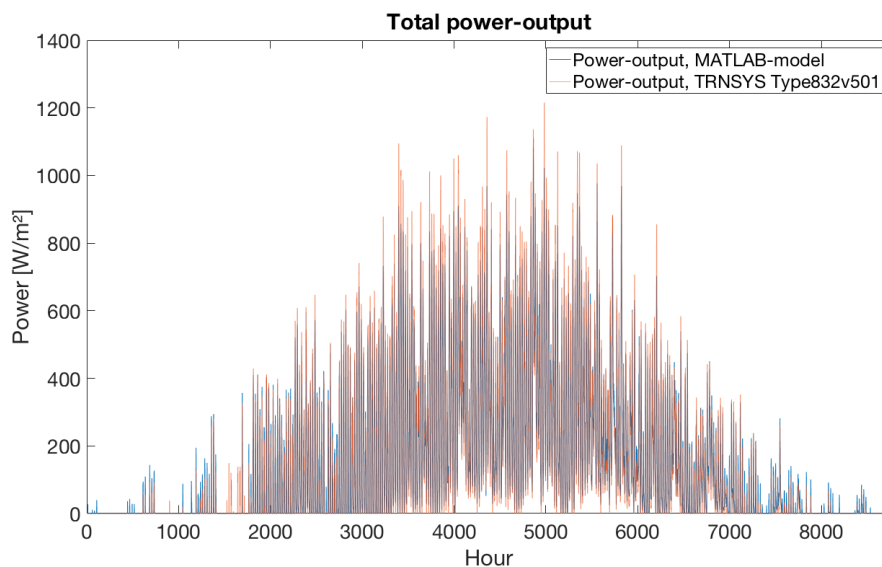


Figure 4.1: Comparison of the models with regards to power-output with weather condition for Arlanda.

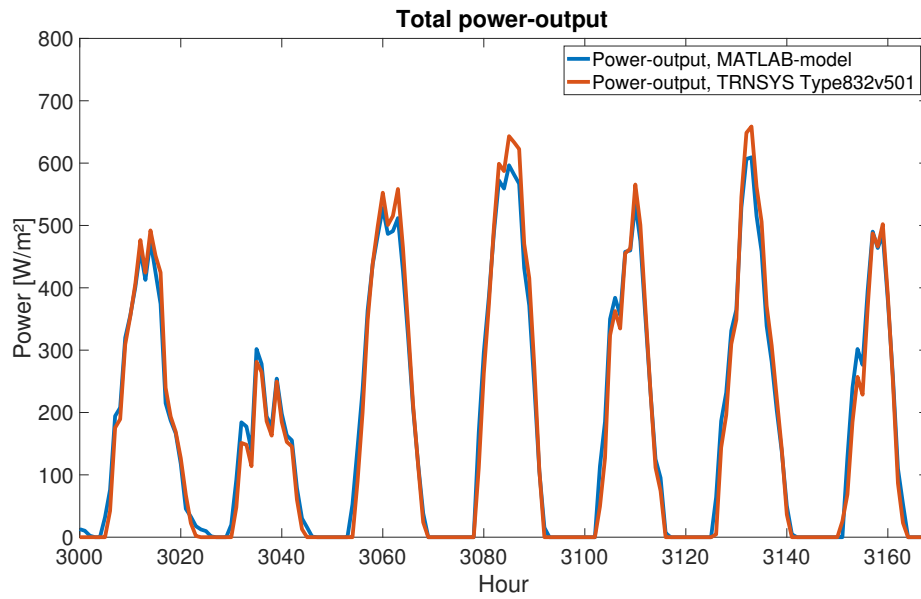


Figure 4.2: Zoomed in view of Figure 4.1 for a week in May.

The total energy gain during a year for different inlet fluid temperatures for the two models are presented in Figure 4.3. The validation shows that the MATLAB-model gives fair values, especially for an inlet temperature up to 12°C, which is the temperature interval the MATLAB-model will be mostly used for. The difference between the energy per year at inlet temperature 12°C for both models is 2%.

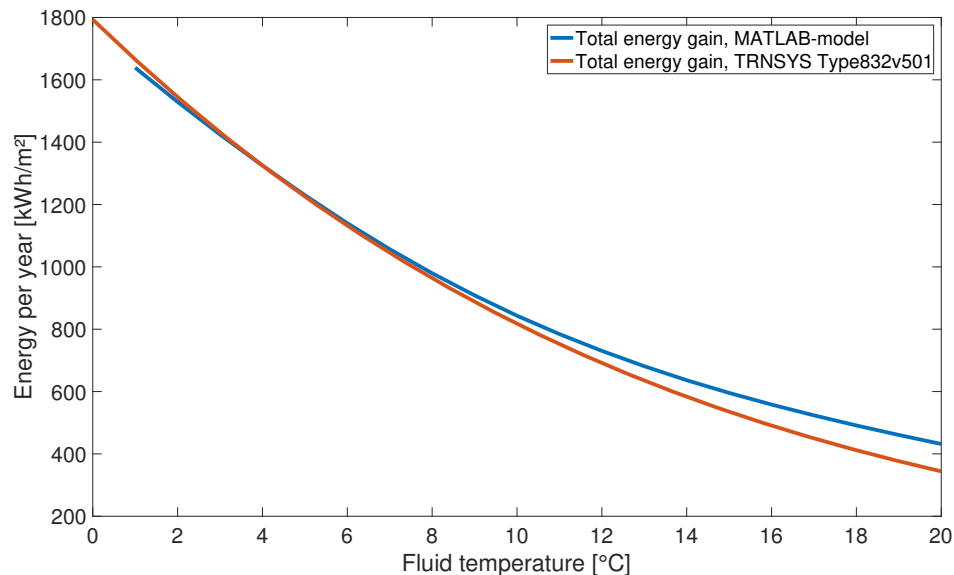


Figure 4.3: Comparison of the energy gain for different inlet temperatures with weather condition for Arlanda.

4.1.2 Implementation of Solar Thermal Collector in Umeå

The low-temperature solar collector is researched to be a part of an energy system with conditions similar to Umeå. How much energy gain the solar collector will give for different inlet temperatures is shown in Figure 4.4. It can be seen that a low-temperature solar collector is the right choice in a temperature interval up to 12 °C. After that temperature there will not be any energy gain from condensation and the convection between the outdoor air will become an energy loss instead of an energy gain.

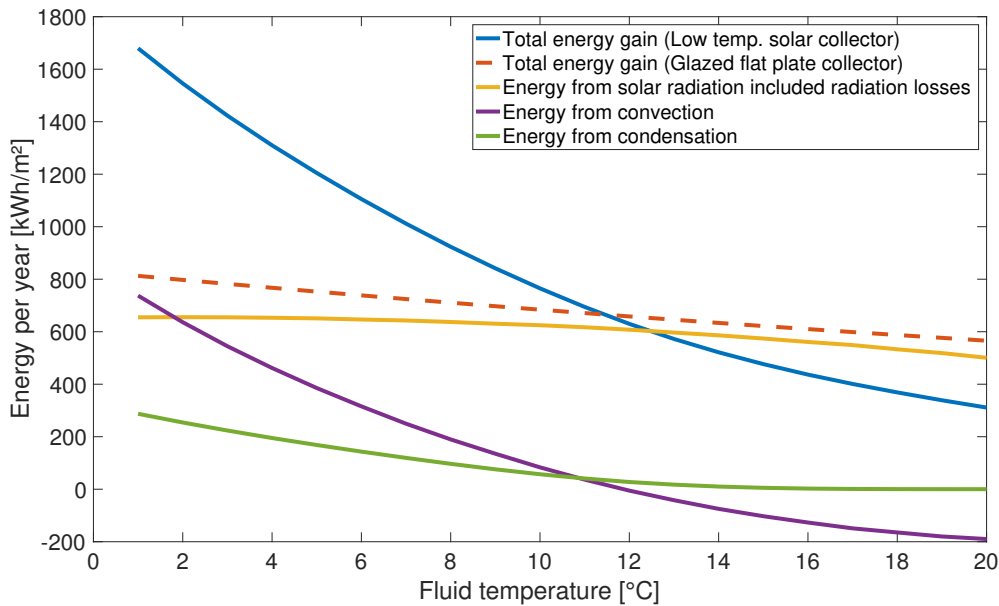


Figure 4.4: Total energy gain from a low-temperature solar collector compared with a glazed flat plate solar collector for different inlet fluid temperature. The plot also shows the contribution from radiation, convection and condensation for the low-temperature solar collector.

The total power-output with conditions similar to Umeå and with a fluid temperature that varies between 0.5 °C in the winter and 26.8 °C in the late summer with a mean value of 6.4 °C is shown graphically in Figure 4.5 and in numbers in table 4.4 in chapter 4.2. The power contribution from solar radiation over the year is shown in Figure 4.6, the power contribution from condensation is shown in Figure 4.8 and the power contribution from convection is shown in Figure 4.7. If the total power from the low-temperature solar collector is negative, the pump is turned off and the power is set to zero.

Figure 4.9 shows how the temperature between the inlet and outlet will vary for a low-temperature solar collector module of 12 m².

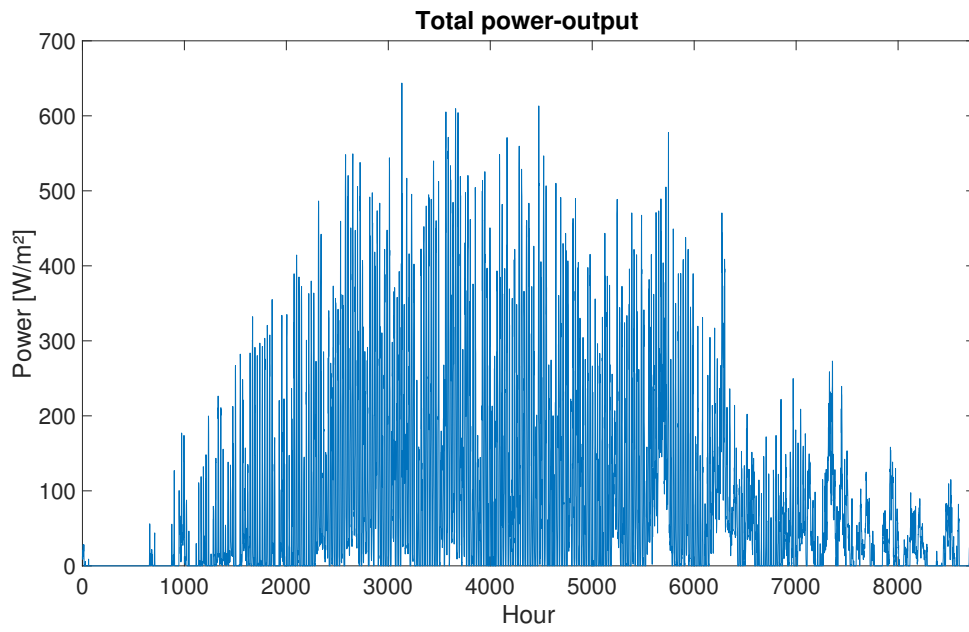


Figure 4.5: The total power-output from a low-temperature solar collector in Umeå.

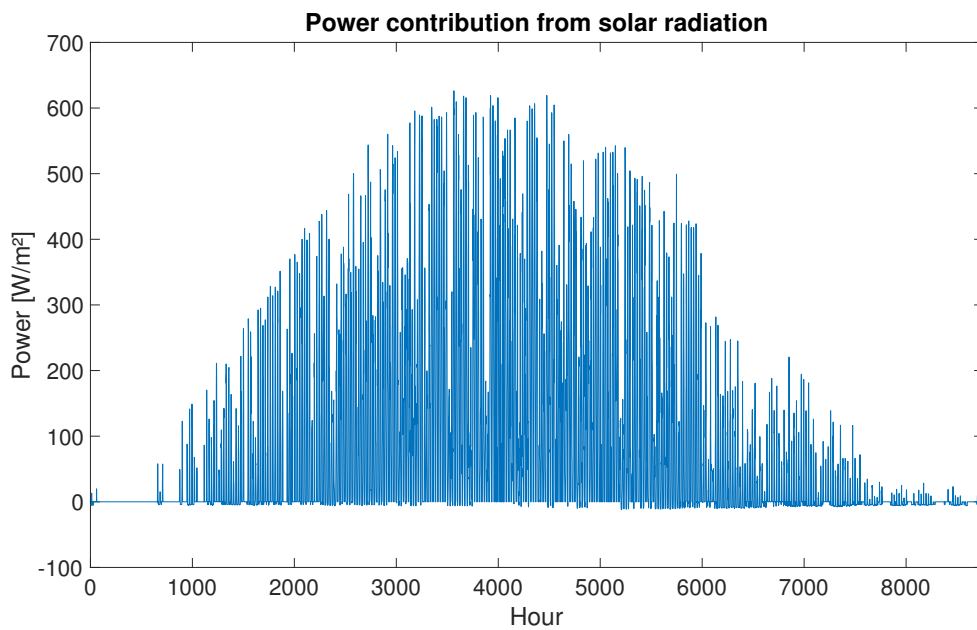


Figure 4.6: The power contribution from solar radiation for a low-temperature solar collector.

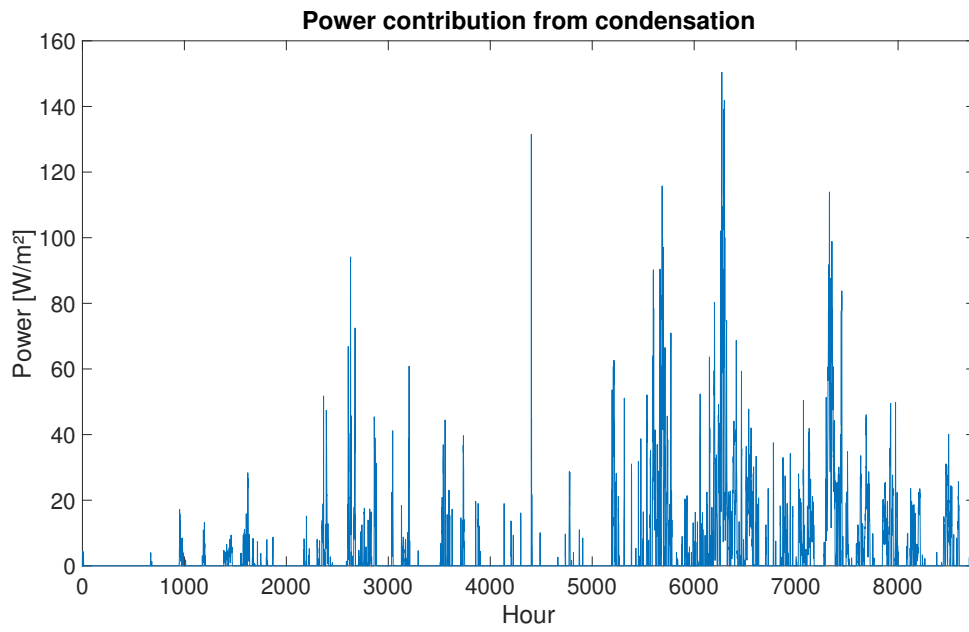


Figure 4.7: The power contribution from condensation for a low-temperature solar collector

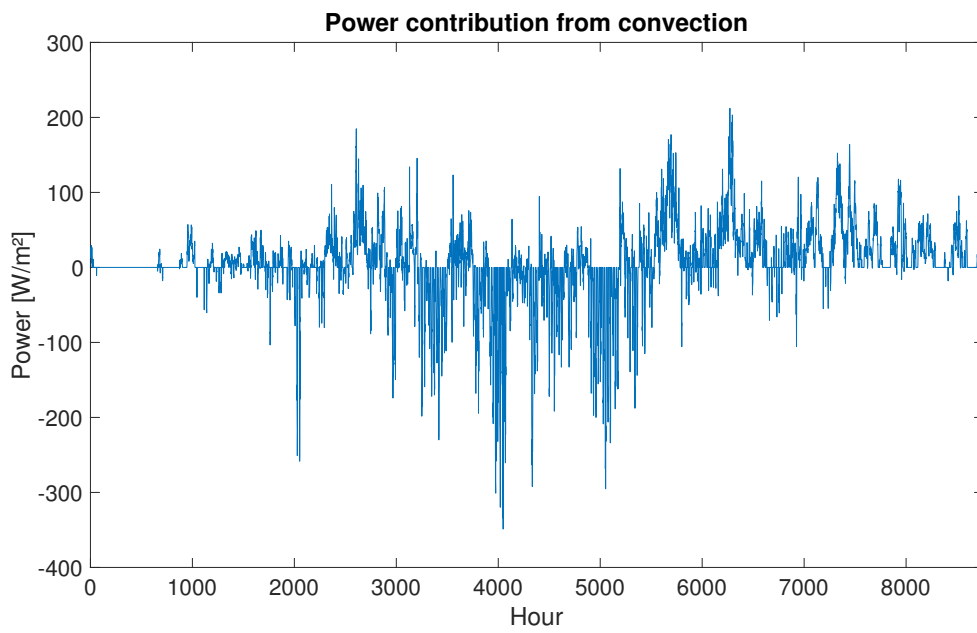


Figure 4.8: The power contribution from convection for a low-temperature solar collector.

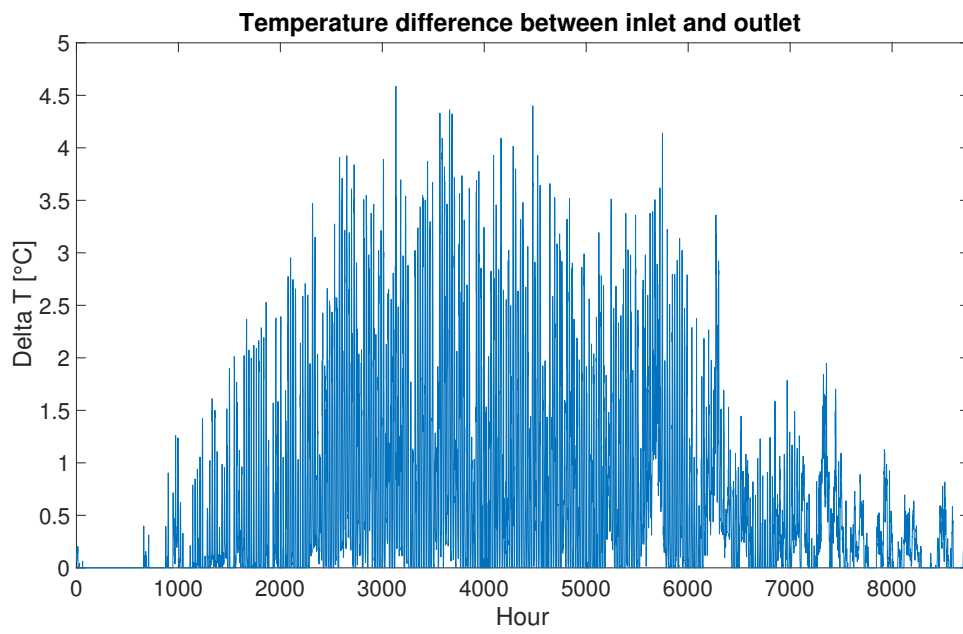


Figure 4.9: ΔT between the inlet and outlet for a low-temperature solar collector module of 12 m².

4.1.3 Sensitivity Analysis

To analyze how sensitive the results from the MATLAB-model are, a sensitivity analysis has been made. The inlet temperature to the low-temperature solar collector is kept constant at 5 °C. The total annual energy gain and the contribution from radiation, convection and condensation are compared for different cases where each hour of the year, the solar irradiance, wind speed, relative humidity is multiplied by a factor of 1.05 or 0.95 separately. Also, how the outdoor temperature affects the result is investigated by adding or subtracting 1 °C. The result of the sensitivity analysis is presented in table 4.1. When multiplying the humidity by a factor of 1.05 the relative humidity will end up over 100% and in this case the relative humidity is set to 100%. This occurs 2037 hours over the year. In the reference case the mean value of the relative humidity is 85.3% and in the case when it is multiplied by 1.05 the mean value becomes 88.9%. When the humidity is multiplied by 0.95 the mean value instead becomes 81.1%.

To analyze how the overall weather condition affects the result, the energy gain for different fluid temperatures for conditions similar to Umeå is compared with weather conditions similar to Stockholm and Gothenburg, see Figure 4.4. The mean value for temperature, solar irradiance, wind speed and humidity for the different cases are presented in table 4.2. The results with conditions similar Stockholm is presented in Figure 4.10 and Gothenburg in Figure 4.11. As can be seen in the figures the total energy gain from the low-temperature solar collector becomes larger with a warmer climate similar Gothenburg. It is particularly the contribution from the convection that increase in the Gothenburg case.

Table 4.1: Sensitivity analysis for how the different weather parameters affect the total energy gain and the contribution from radiation, convection and condensation.

Changing parameter	Total [kWh/m ²]	Radiation [kWh/m ²]	Convection [kWh/m ²]	Condensation [kWh/m ²]
Reference case	1196.8	650.8	379.8	166.2
Solar irradiance * 1.05	1229.4	686.5	377.2	165.8
Solar irradiance * 0.95	1164.2	615.6	382.1	166.5
Wind speed * 1.05	1216.2	650.3	393.1	172.8
Wind speed * 0.95	1177.1	651.7	365.9	159.5
Temperature + 1°C	1312.0	655.1	453.9	203.0
Temperature - 1°C	1086.5	636.6	316.0	133.9
Humidity * 1.05	1219.4	649.8	378.8	190.9
Humidity * 0.95	1171.4	652.0	381.1	138.4

Table 4.2: Mean values for the different weather parameters that affect the solar collector.

Conditions	Temperature [°C]	Radiation [W/m ²]	Wind [m/s]	Humidity [%]
Umeå	6.1	101.1	4.8	85.3
Gothenburg	9.2	112.1	4.2	78.2
Stockholm	8.1	115.1	4.1	84.4

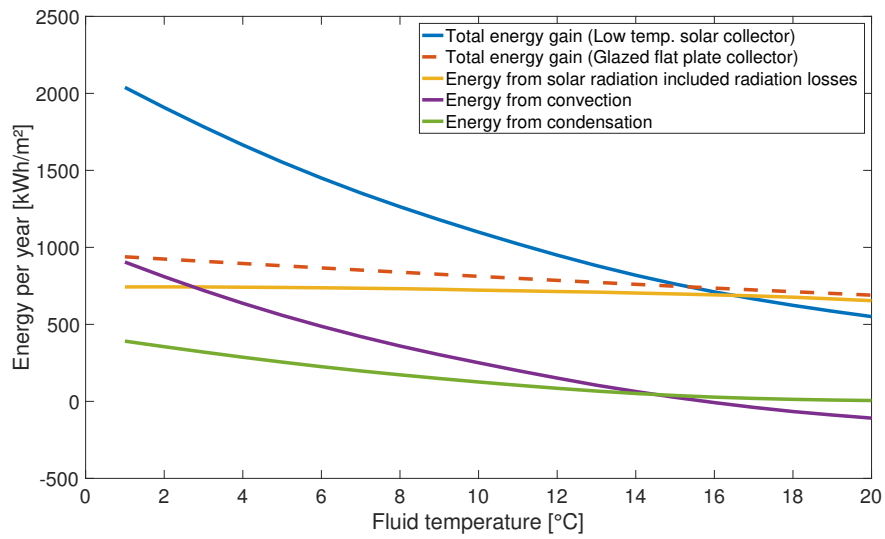


Figure 4.10: Energy for different inlet temperatures with weather condition like Stockholm.

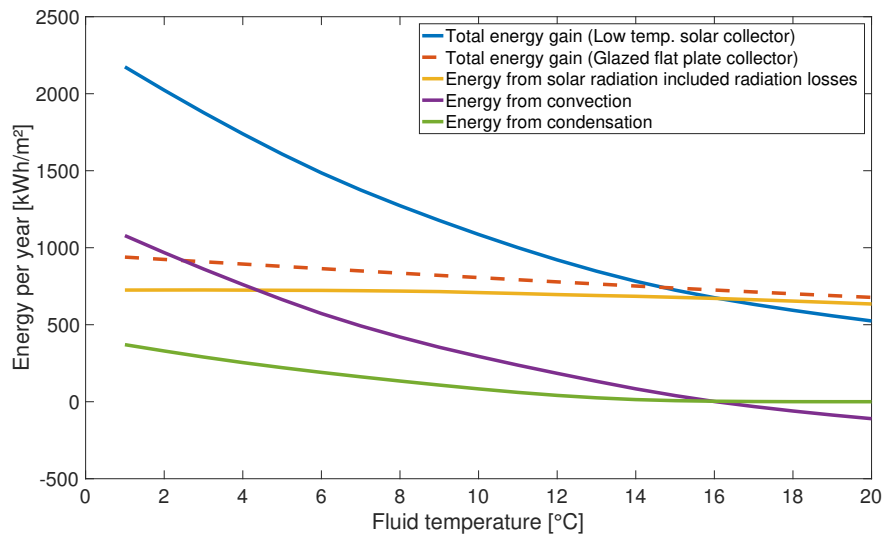


Figure 4.11: Energy for different inlet temperatures with weather condition like Gothenburg.

4.1.4 Cost of Low-Temperature Solar Collector

The total investment cost for a low-temperature solar collector is presented in table 4.3. The cost of the collector tubes, including the installation and liquid inside is assumed to be 500 SEK/m². There will also be an additional cost for the parallel connection between the modules. This cost will vary depending on the size of the collector, with a larger area of collectors the distances for connecting the modules become longer. The cost of the pipes between the roof and the energy space also depends on the size of the solar thermal collector. A larger size of the solar thermal collector leads to a larger flow, which needs a larger diameter of the pipe. The cost of the pipe including the installation is between 3000 and 5400 SEK/m, the cost includes the return pipe, so the distance should be between A and B. Because the liquid in the solar collector needs to cope with very cold and hot temperatures there will be an own circuit for the solar collector with a special liquid for them. The installation therefore needs a heat exchanger. This heat exchanger is assumed to cost 60 000 SEK. The pump for the system needs to handle the pressure drop. The pressure drop over the low-temperature solar collector module of 12 m² is 40 kPa. These modules are connected in parallel so the flow of the fluid will increase by 0.4 l/s for each module. The pressure drop in the pipe between the collector and the energy space is assumed to be 100 Pa/m.

Table 4.3: Investment cost for a low-temperature solar thermal collector.

Size of solar thermal collector [m ²]	Collector modules, including installation and liquid [SEK]	Pipes between energy space and roof, including installation and heat exchanger [SEK]	Pump cost [SEK]	Total investment cost [SEK]
60	37 500	150 000	8 500	196 000
120	76 000	156 000	16 500	248 500
180	115 500	162 000	22 425	299 925
240	156 000	168 000	24 375	348 375
300	197 500	174 000	24 375	395 875
360	240 000	180 000	24 375	444 375
420	283 500	186 000	27 300	496 800
480	328 000	192 000	27 300	547 300
540	373 500	198 000	27 300	598 800
600	420 000	204 000	27 300	651 300
660	467 500	210 000	28 275	705 775
720	516 000	216 000	28 275	760 275
780	565 500	222 000	28 275	815 775
840	616 000	228 000	28 275	872 275
900	667 500	234 000	28 275	929 775

4.2 Potential Savings in Investment Cost with Low-Temperature Solar Collector

To be able to examine the potential savings in investment cost with a low-temperature solar collector the energy output for each hour is calculated with the MATLAB-model. The inlet temperature varies between 0.5 °C in the winter and 26.8 °C in the late summer with a mean value of 6.4 °C. The energy output per square meter each month is presented in table 4.4. The table also shows the contribution from radiation, convection and condensation. The weather conditions are previously presented in table 3.1. The temperature before the BTES without solar collector and with 360 m² solar collector is presented in Appendix C. The heat extraction and borehole depth for these two cases is also presented in Appendix C.

Table 4.4: Energy output every month from a low-temperature solar collector.

Month	Total energy output [kWh/m ²]	Energy contribution radiation [kWh/m ²]	Energy contribution convection [kWh/m ²]	Energy contribution condensation [kWh/m ²]
January	0.90	0.41	0.45	0.04
February	13.72	10.44	2.89	0.39
March	47.22	47.39	-0.88	0.70
April	97.71	79.61	15.19	2.91
May	117.15	126.11	-10.24	1.28
June	105.19	127.58	-22.96	0.57
July	94.92	116.12	-21.75	0.55
August	103.20	84.91	11.24	7.04
September	71.95	39.12	22.79	10.04
October	31.46	13.85	13.84	3.77
November	37.39	1.38	26.83	9.18
December	13.88	-1.07	12.44	2.50
Total	734.68	645.86	49.84	38.98

The energy output each hour from the low-temperature solar collector is subtracted from the energy affecting the BTES in table 3.2. This gives a new required borehole length calculated by EED. The required borehole length and the corresponding cost are presented in table 4.5. The borehole investment cost is assumed to be 300 SEK/m [13]. The savings compared to not have any low-temperature solar collector at all is also presented in the table. The result is shown graphically in Figure 4.12. The reason why the required borehole length increase after 250 m² of low-temperature solar collector is that the BTES needs to be dimensioned so that the fluid temperature not exceed 25 °C.

4. RESULTS

Table 4.5: Required borehole length according to EED and the cost savings with a low-temperature solar collector.

Size of solar thermal collector [m ²]	Required borehole length [m]	Borehole thermal energy storage cost [SEK]	Cost savings compared to no solar thermal collector [SEK]
0	24 243	7 272 900	0
60	23 639	7 091 700	-14 800
120	22 744	6 823 200	201 200
180	21 898	6 569 400	403 575
240	21 357	6 407 100	517 425
300	21 355	6 406 500	470 525
360	21 780	6 534 000	294 525
420	22 298	6 689 400	86 700
480	22 810	6 843 000	-117 400

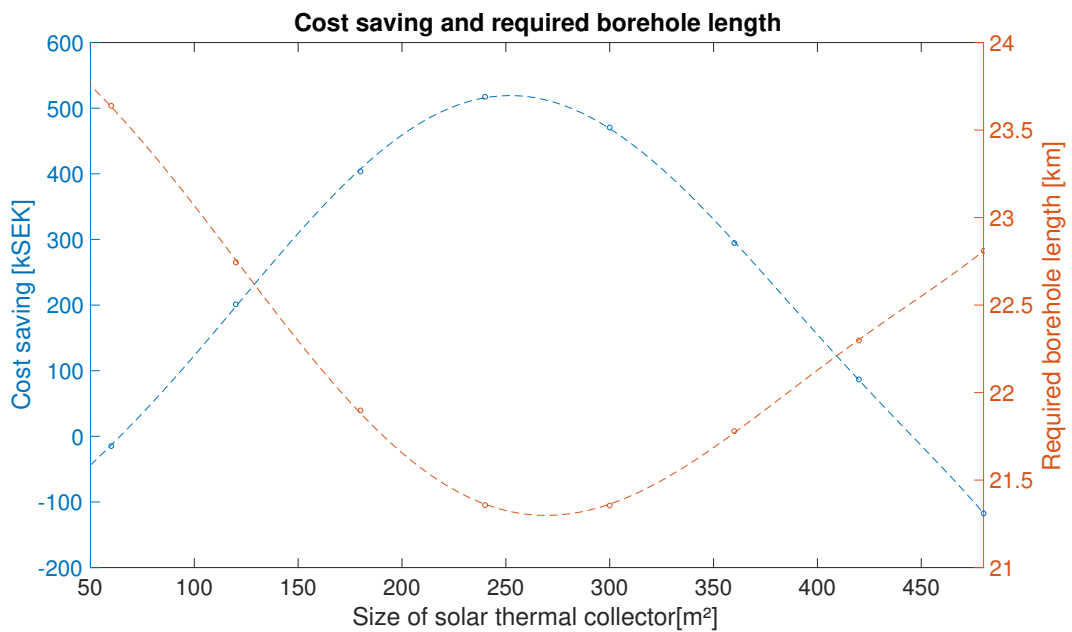


Figure 4.12: Required borehole length according to EED and the cost savings with a low-temperature solar collector.

In the examined case there is a large cooling demand during summer, so the recharge of the BTES is already large during this period. Therefore, it is examined how the system will be affected if the low-temperature solar collector is not operating during June, July and August. The result is shown in table 4.6. The result is shown graphically in Figure 4.13.

The results show that with a small low-temperature solar collector it is best to use the collector all year around, but when the size is larger than 240 m² it is beneficial to turn off the low-temperature solar collector or use it for something else like heating a swimming pool. The combined graph with the low-temperature solar collector operating all year around until a size of 240 m² and for larger size operating without June, July and August is shown in Figure 4.14. In this specific case it is possible to save up to 669 525 SEK in investment cost.

Table 4.6: Required borehole length according to EED and the cost savings with a low-temperature solar collector, no operation of the solar collector during June, July and August.

Size of solar thermal collector [m ²]	Required borehole length [m]	Borehole thermal energy storage cost [SEK]	Cost savings compared to no solar thermal collector [SEK]
0	24 243	7 272 900	0
60	23 718	7 115 400	-38 500
120	23 002	6 900 600	123 800
180	22 370	6 711 000	261 975
240	21 861	6 558 300	366 225
300	20 935	6 280 500	596 525
360	20 530	6 159 000	669 525
420	20 585	6 175 500	600 600
480	20 658	6 197 400	528 200
540	20 742	6 222 600	451 500
600	20 902	6 270 600	351 000
660	21 097	6 329 100	238 025
720	21 270	6 381 000	131 625
780	21 431	6 429 300	27 825
840	21 572	6 471 600	-70 975
900	21 731	6 519 300	-176 175

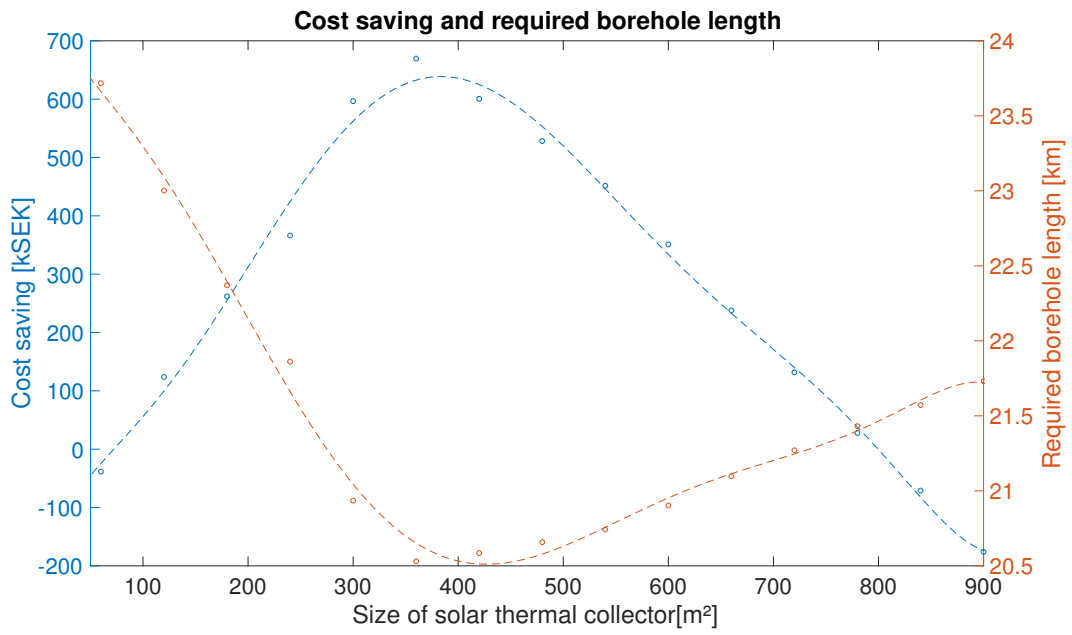


Figure 4.13: Required borehole length according to EED and the cost savings with a low-temperature solar collector, assuming no operation of the solar collector during June, July and August.

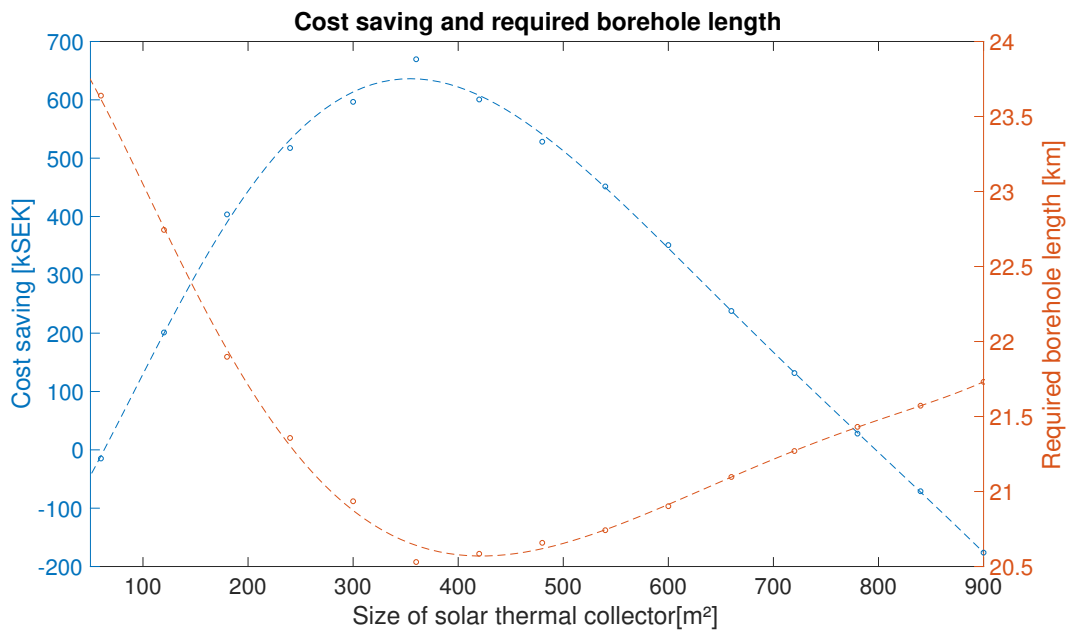


Figure 4.14: Required borehole length according to EED and the cost savings with low-temperature solar collector, if more than 240 m² solar collector is present there will be no operation of the solar collector during June, July and August.

5 Discussion

This chapter clarifies and questions the method and the results. It also explains how the result can be used and if there are any other way to use the low-temperature solar collector. The advantages and challenges with a system using BTES and low-temperature solar collector is discussed.

5.1 Model of Low-Temperature Solar Collector

The annual performance of a low-temperature solar collector under these operating conditions is above 700 kWh/m^2 , see table 4.4. As can be seen in chapter 4.1.3 it is possible to collect even more energy with a higher temperature and more humid climate. The graph in Figure 4.3 shows that the model that are made for a low-temperature solar collector gives a fair estimated value for the energy output, in the temperature interval where it will be used most of the time.

The low-temperature solar collector works even when there is no solar radiation, due to the heat transfer through convection and condensation. There is a risk that condensation water penetrate into the house and roof construction which must be taken into account. It's also important to avoid cooling the roof that much that the air on the inside condensate and create dampness.

In the winter there will also be situation of frost on the collector surface. That is not taken to account in the model. This will increase the energy output by adding the phase change energy when freezing. But it will also lead to that the collector needs to be defrosted to keep a good performance. In winter there will also be snow covering the collector which must be removed to maintain the performance.

An uncertain factor is the wind. The winds on the collector plane depends on the building and the environment around. To get a more accurate model, the wind speed on the roof should be measured instead of taking the data from SMHI. The data from SMHI is measured 10 m above the ground and then equation 3.10 is used to calculate the wind speed on the collector plane.

The MATLAB-model uses the properties of water to calculate the heat transfer trough the internal flow. In reality a mixture for solar collectors will be used to prevent freezing and vaporization inside the collector. A common mixture is water and glycol. Glycol is 5-10% less efficient than water in transferring heat. However, glycol will reduce dirt and corrosion that can reduce heat transfer in the long term.

5.2 Integration with EnergyMachines™ and Borehole Thermal Energy Storage

The integration between a low-temperature solar collector, EnergyMachines™ and BTES leads to that the inlet temperature into the collector could be kept at a low temperature all year around, which leads to a high energy output from the low-temperature solar collector.

In this specific case the energy output from the low-temperature solar collector reduces the size of the BTES that much so the investment cost decreases with 669 525 SEK. The building that has been investigated has a quite large cooling demand. It would have been interesting to do the research on a building with a small cooling demand compared to the heating demand. In that case the savings could be even larger, there is then also a possibility to "overheat" the BTES, which decreases the temperature lift that the heat pump needs to do in heating mode. By doing that the electricity consumption will decrease. Below is the advantages and challenges with a low-temperature solar collector stated.

Advantages

- By using a low-temperature solar collector it is possible to lower the investment cost for the entire energy system which gives a shorter payback time.
- Low-temperature solar collectors make it possible to fulfill the energy demand with less borehole meters and volume of BTES.
- Instead of turning off the low-temperature solar collector during summer there is also an opportunity to preheat tap water or to heat for example swimming pools.
- If there is a shortage of water, it is possible to collect the condensate.
- Low-temperature solar collectors are easy to implement to an existing storage if it is under-dimensioned or if the heating demand becomes larger in the future.
- For buildings with high heating demand there is a possibility to "overheat" the BTES to make the temperature lift smaller during heating operation which results in less electricity consumption.

Challenges

- Low-temperature solar collectors will need roof space and there are people that think the collector is not aesthetically appealing. The construction also needs to be able to handle the extra load caused by the low-temperature solar collector.
- There will be more components that could break.
- There is a risk of dampness if it is not taken into account during projection.
- The construction needs to be able to handle the snow-load and to maintain the performance the snow covering the collector must be removed.

6 Conclusion

The main aim of this thesis was to dimension an integrated energy system where a low-temperature solar collector is connected to an EnergyMachines™ and BTES. The results show that in this specific case, the most cost effective solution is to install 360 m² low-temperature solar collector that is not operating in June, July and August. How big area of low-temperature solar collector that are most profitable depends on the heating and cooling demand, so a new investigation must be done for each project to calculate the optimal area of the low-temperature solar collector.

The objectives, chapter 1.2, also consists of two other questions. Firstly, how the heat from the low-temperature solar collector should be stored. Should it be stored in the BTES or used directly in the evaporator? To gain as much energy as possible from the low-temperature solar collector the inlet-temperature should be as low as possible. In spring, autumn and winter the temperature of the fluid is lowest before entering the BTES. In summertime the temperature is lowest after the BTES, but in this case the cooling demand is greater than the heating, so there is no need to heat the collector fluid before the EnergyMachines™. So the fluid before the BTES is also used during summer, for a low-temperature solar collector with an area smaller than 300 m².

Secondly, the thesis answered how the low-temperature solar collector will affect the price per kWh heat. In this case when the COP is kept constant and the low-temperature solar collector is replacing a part of the BTES, the electricity consumption is the same as when not having a low-temperature solar collector so the price per kWh heat for the costumer will not change. The benefit with an energy system consisting of a low-temperature solar collector is that the investment cost could decrease, which mean a shorter payback time.

To be able to faster calculate the optimal area of a solar collector for a building, the next step is to build a model for the BTES, instead of the EED-model that is used. If these two models are built together, it will save a lot of time when calculating the optimal collector area. Today the iteration for different areas of low-temperature solar collector needs to be done manually and then the different energy demand corresponding to the collector area is taken as input data to the EED-model.

Further, the model should be integrated with a model of the EnergyMachines™ to be able to calculate the electricity savings that can be done by "overheating" the BTES. This is especially interesting for buildings with a high heating demand.

It would be interesting to compare the result for the low-temperature solar collector with a photovoltaic thermal hybrid solar collector that generates both heat and electricity. When using a hybrid solar collector it is possible to reduce the electricity that has to be purchased.

References

- [1] LLC Underground Energy. *BTES - Borehole Thermal Energy Storage*. 2009. URL: <http://www.underground-energy.com/BTES.html> (visited on 05/18/2017).
- [2] LLC Underground Energy. *ATES - Aquifer Thermal Energy Storage*. 2009. URL: <http://www.underground-energy.com/ATES.html> (visited on 05/18/2017).
- [3] Elisabeth Kjellsson. *Solar Collectors Combined with Ground-Source Heat Pumps in Dwellings-Analyses of System Performance*. Vol. 1018. Byggnadsfysik LTH, Lunds Tekniska Högskola, 2009.
- [4] Giuseppe Emmi et al. "Solar assisted ground source heat pump in cold climates". In: *Energy Procedia* 82 (2015), pp. 623–629.
- [5] Karolis Januševičius and Giedrė Streckienė. "Solar Assisted Ground Source Heat Pump Performance in Nearly Zero Energy Building in Baltic Countries". In: *Scientific Journal of Riga Technical University. Environmental and Climate Technologies* 11 (2013), pp. 48–56.
- [6] Energiförbättring Väst AB. *Referenser*. URL: <http://efvab.se/referenser> (visited on 02/03/2018).
- [7] William Steel. *Novel Hybrid Solar PV-Geothermal Energy System Piloted in Sweden*. 2016. URL: <http://www.renewableenergyworld.com/articles/2016/09/novel-hybrid-solar-pv-geothermal-energy-system-piloted-in-sweden.html> (visited on 02/03/2018).
- [8] Jan-Olof Dalenbäck. *Senior researcher at Chalmers University of Technology*. Personal communication. Feb. 2, 2018.
- [9] Nexion. *Referenser*. URL: <https://www.nexion.se/referenser/> (visited on 02/03/2018).
- [10] Norconsult. *Sveriges mest energieffektiva yrkesskola*. 2017. URL: <https://www.norconsult.se/vara-projekt/sveriges-mest-energieffektiva-yrkesskola/> (visited on 02/03/2018).
- [11] Theodore L. Bergman & Adrienne S. Lavine. *Principles of Heat and Mass Transfer*. 2nd ed. John Wiley Sons, 2012. ISBN: 9780470646151.
- [12] Energy Machines Sweden AB. *Kyl- och värmepumpsystem, produktfolder*. 2016.
- [13] Hans-Göran Göransson. *CTO at Energy Machines Sweden AB*. Personal communication. Sept. 1, 2017.
- [14] Mikael Erlström et al. *Geologisk information för geoenergianläggningar—en översikt*. 2016.
- [15] Lars Börjesson. *Utvärdering och optimering av bergvärmesystemet vid kv. Barnfröken*. 2005.
- [16] Annelie Karlsson et al. *Borrhåls-och grundvattenlager. Praktisk handbok om geoenergi*. 2012.
- [17] Lena Gunnarsson et al. *Solenergi - Hållbart & gratis!* 2015.
- [18] Elisabeth Kjellsson. *Solvärme i bostäder med analys av kombinationen solfångare och bergvärmepump*. 2004.
- [19] Svensk Solenergi. *Solvärme, kostnader - Vad kostar ett solvärmesystem?* URL: <http://www.svensksolenergi.se/fakta-om-solenergi/fragor-och-svar/solvaerme-kostnader> (visited on 09/21/2017).
- [20] Svensk Solenergi. *Hur fungerar en poolsolfångare?* URL: http://www.svensksolenergi.se/fakta-om-solenergi/fragor-och-svar#Hur_fungerar_en_poolsolfangare (visited on 10/03/2017).
- [21] Svensk Solenergi. *Vakuumsolfångare - Hur fungerar en vakuumsolfångare?* URL: <http://www.svensksolenergi.se/fakta-om-solenergi/fragor-och-svar/vakuumsolfangare> (visited on 09/21/2017).

- [22] Svensk Solenergi. *Plana solfångare - Hur fungerar en plan solfångare?* URL: <http://www.svensksolenergi.se/fakta-om-solenergi/fragor-och-svar/plana-solfangare> (visited on 09/21/2017).
- [23] Fabio Struckmann. *Analysis of a flat-plate solar collector*. 2008.
- [24] Göran Wall. *Naturliga fysiska resurser och Livskraftiga energisystem*. 1997.
- [25] Jan Erik Nielsen. *European Solar Thermal Industry Federation, Collector efficiency*. 2006.
- [26] Clemens Schwingshackl et al. *Wind effect on PV module temperature: Analysis of different techniques for an accurate estimation*. 2013.
- [27] Bengt Perers. *Senior researcher at Technical University of Denmark*. Personal communication. Nov. 8, 2017.
- [28] Isidoro Martinez. *Thermo Optical Properties*. URL: <http://webserver.dmt.upm.es/~isidoro/dat1/Thermooptical.pdf> (visited on 10/17/2017).
- [29] Sveriges meteorologiska och hydrologiska institut. *Meteorologiska Observationer*. URL: <http://opendata-download-metobs.smhi.se/explore/?parameter=9> (visited on 10/18/2017).

Appendix A MATLAB

```
1  %-----
2  %-----
3  % Low-temperature solar collector
4  % Written by: Alexander Malmberg
5  % Date: 2017-11-14
6  %-----
7  %-----
8  clc
9  clear all
10 format long
11 mode=1; %1=Power and energy, one year
12 %Indata Unglazed collector %2=How the fluidtemp. affect the energy
13 A_solar=12; %Surface area of the solar collector [m2]
14
15 %Indata Collector tube for low-temp solar collector
16 Di=0.035; %Inside diameter [m]
17 Do=0.04; %Outside diameter [m]
18 epsilon_tube=0.1; %Emissivity,
19 alpha_tube=0.9; %Selective absorvity
20 k_tube=0.19; %Conductivity PVC [W/mK]
21 space_between=0.03; %Space between tubes [m]
22 p_fluid=1; %Pressure inside tubes [bar]
23
24 %-----
25 %Indata Flat plate solar collector
26 n0=0.78; %Optical efficiency
27 a1=3.2; %Linear heat loss coefficient
28 a2=0.015; %Quadratic heat loss coefficient
29
30 %-----
31 %Constants
32 sigma=5.670367*10^-8; %Stefan Boltzmann constant [W/m2K4]
33
34 %Air outside [SMHI-data]
35 data_solar=xlsread('Indata.xlsx',2);
36 data_temp=xlsread('Indata.xlsx',3);
37 data_hum=xlsread('Indata.xlsx',4);
38 data_wind=xlsread('Indata.xlsx',5);
39
40 wind=data_wind(1:8760,2); %Wind collector [m/s]
41 T_a=data_temp(1:8760,2); %Air temp. [C]
42 humidity=data_hum(1:8760,2); %Relative humidity [%]
43 G=data_solar(1:8760,2); %Solar irradiance [W/m2]
44 T_sky=-10; %Effective sky temp. [C], page 825
45 p=101.3*10^3; %Air-pressure [Pa]
46
47 %Temp and flow
48 if mode==1
49     data_fluid=xlsread('Indata.xlsx',1);
50     v_fluid=data_fluid(1:8760,3); %Make array of Fluid flow [m3/s]
51     T_fluid=data_fluid(1:8760,2); %Make array of Start fluid temp. [C]
52     T_fluid_2=T_fluid;
53     n=20; %Number of pieces the collectortube is divedid in to
```

A. MATLAB

```
54 Energy_low_temp_month=zeros(1,12);
55 Energy_low_temp_solar_month=zeros(1,12);
56 Energy_flat_month=zeros(1,12);
57 Energy_low_temp_cond_month=zeros(1,12);
58 Energy_low_temp_conv_month=zeros(1,12);
59 else
60     flow_fluid=0.0005;           %Fluid flow [m3/s]
61     Temp_start=1;               %Min inlet fluid temperature [C]
62     Temp_end=20;               %Max inlet fluid temperature [C]
63     v_fluid=ones(8760,1)*flow_fluid; %Make array of fluid flow [m3/s]
64     T_fluid=ones(8760,1)*Temp_start; %Make array of start fluid temp.[C]
65     T_fluid_2=T_fluid;
66     n=5; %Number of pieces the collectortube is divedid in to
67     Sum_energy_total_kwh=zeros(1,length(Temp_end));
68     Sum_energy_radiation_kwh=zeros(1,length(Temp_end));
69     Sum_energy_flat_kwh=zeros(1,length(Temp_end));
70     Sum_energy_conv_kwh=zeros(1,length(Temp_end));
71     Sum_energy_cond_kwh=zeros(1,length(Temp_end));
72 end
73
74 %-----
75 %Low temperature solar collector
76 %-----
77 %Calculate Length and area of one node
78 L=A_solar/((Do+space_between)*n); %Length of one piece to get desired area
79 A=L*pi*Do;                         %Outside area of tubes
80 A_inside=pi*(Di/2)^2;              %Cross-section area of tubes
81
82 %Make vectors for faster simulation
83 Q_tot_radiation_low=zeros(1,length(T_a));
84 Q_tot_unglazed=zeros(1,length(T_a));
85 Q_tot_condensation_low=zeros(1,length(T_a));
86 Q_tot_convection_low=zeros(1,length(T_a));
87 Q_flat=zeros(1,length(T_a));
88 T_fluide_out_collector=zeros(1,length(T_a));
89 T_fluid_out_flat=zeros(1,length(T_a));
90 W_coll=zeros(1,length(T_a));
91 Q_tot_low=zeros(1,length(n));
92 Q_conv=zeros(1,length(n));
93 Q_cond=zeros(1,length(n));
94 Q_radiation=zeros(1,length(n));
95
96 if mode==1 %Mode 1
97     for i = 1:length(T_a)
98         if T_a(i)>0
99             tick=1;
100            while n+1>tick
101                %Calculate wind speed in collectorplane
102                W_coll(i)=wind(i)*0.68-0.5;
103                if W_coll(i)<0
104                    W_coll(i)=0;
105                end
106
107                %Calculate h_convetion, Bengt Peres
108                h_conv=2.8+3*W_coll(i);
109
110                %Calcualte energy from condensation, Bengt Peres
```

```
111         T_s=T_fluid(i);
112         rho_air=f_air_density2(T_a(i),humidity(i),p); % [kg/m3]
113         humidity_ratio=convert_humidity(p,T_a(i)+273.15,...
114             humidity(i), 'relative humidity','specific humidity');
115         v_air=rho_air*humidity_ratio; % [kg/m3]
116         v_sat=0.001*(4.85+0.347*T_s+0.00945*T_s^2+0.000158*...
117             T_s^3+0.00000281*T_s^4);
118         Cp_air=1.005*10^3; % (kJ/(kg K))
119         rw=2260*10^3; %Energy for the phase change
120
121         q_condensation=rw*(h_conv/(rho_air*Cp_air))*(v_air-v_sat);
122
123         %Define if there will be condensation or not
124         if q_condensation>0
125             Q_cond(tick)=q_condensation*A_solar/n;
126             T_condensation_air=convert_humidity (p, T_a(i)+...
127                 273.15, humidity(i), 'relative humidity',...
128                 'dew point')-273.15; %[C]
129             T_s=T_condensation_air;
130         else
131             Q_cond(tick)=0;
132             T_s=T_fluid(i);
133         end
134
135         %-----
136         %Calculate h_inside, page 549
137         mu_inside=XSteam('my_pT',p_fluid,T_fluid(i));
138         if T_s>0
139             mu_surface=XSteam('my_pT',p_fluid,T_s);
140         else
141             mu_surface=mu_inside;
142         end
143
144         rho_inside=XSteam('rhoL_T',T_fluid(i));
145         Cp_inside=XSteam('CpL_T',T_fluid(i))*10^3; %[J/kgK]
146         k_inside=XSteam('tcL_T',T_fluid(i)); %[W/mK]
147         nu=mu_inside/rho_inside;
148         Re_D=(v_fluid(i)*Di)/(nu*A_inside);
149         Pr=mu_inside*Cp_inside/k_inside;
150
151         if Re_D>10000
152             Nu_D=0.027*Re_D^(4/5)*Pr^(1/3)*...
153                 (mu_inside/mu_surface)^(0.14); %page 567
154         else
155             Nu_D=4.36; %Laminar, uniform q_s, page 567
156         end
157
158         h_inside=Nu_D*k_inside/Di; %page 549
159
160         %-----
161         %Calcualte energy from outdoor temperature diffrence
162         Q_conv(tick)=(T_a(i)-T_fluid(i))/((1/(h_conv*2*pi*L*...
163             (Do/2)))+(log((Do/2)/(Di/2))/(k_tube*2*pi*L))+...
164             (1/(h_inside*2*pi*L*(Di/2)))); %page 136
165
166         %-----
167         %Calcualte energy from Radiation, page 825
```

```
168         alpha_sky=epsilon_tube;
169         q_rad=alpha_tube*G(i)-(epsilon_tube*sigma*...
170             ((T_s+273.15)^4-(T_sky+273.15)^4));
171         Q_radiation(tick)=q_rad*A/2;
172
173         %Calculate total energy
174         Q_tot_low(tick)=Q_cond(tick)+Q_conv(tick)+...
175             Q_radiation(tick);
176
177         %Calculate temperature
178         T_fluid_out=Q_tot_low(tick)/(v_fluid(i)*rho_inside*...
179             Cp_inside)+T_fluid(i);
180         T_fluid(i)=T_fluid_out;
181
182         tick=tick+1;
183     end
184
185     %Sum energy
186     Q_tot_unglazed(i)=sum(Q_tot_low);
187     Q_tot_radiation_low(i)=sum(Q_radiation);
188     Q_tot_condensation_low(i)=sum(Q_cond);
189     Q_tot_convection_low(i)=sum(Q_conv);
190
191     if Q_tot_unglazed(i)>0
192         Q_tot_unglazed(i)=Q_tot_unglazed(i);
193         Q_tot_radiation_low(i)=Q_tot_radiation_low(i);
194         Q_tot_condensation_low(i)=Q_tot_condensation_low(i);
195         Q_tot_convection_low(i)=Q_tot_convection_low(i);
196         T_fluide_out_collector(i)=T_fluid_out;
197     else % Turn of solar collector if Q>0
198         Q_tot_unglazed(i)=0;
199         Q_tot_radiation_low(i)=0;
200         Q_tot_condensation_low(i)=0;
201         Q_tot_convection_low(i)=0;
202         T_fluide_out_collector(i)=T_fluid_2(i);
203     end
204 else
205     Q_tot_unglazed(i)=0;
206     Q_tot_radiation_low(i)=0;
207     Q_tot_condensation_low(i)=0;
208     Q_tot_convection_low(i)=0;
209     T_fluide_out_collector(i)=T_fluid_2(i);
210 end
211
212 T_fluid(i)=T_fluid_2(i); %Reset fluid-temperature
213
214 %Calculate Rho and cp for the fluid inside solar collector
215 rho_inside=XSteam('rhoL_T',T_fluid_2(i));
216 Cp_inside=XSteam('CpL_T',T_fluid_2(i))*10^3; %[J/kgK]
217
218 %-----
219 %Flat plate solar collector, see "Solvarme i bostader med analys
220 %av kombinationen solfangare och bergvarmepump"
221 %-----
222 eta_flat= (G(i)*n0-a1*(T_fluid_2(i)-T_a(i))-a2*...
223             ((T_fluid_2(i)-T_a(i))^2))/G(i);
224 if 1000>eta_flat && eta_flat>0 && eta_flat~=-inf
```

```

225         Q_flat(i)=eta_flat*G(i)*A_solar;
226         T_fluid_out_flat(i)=Q_flat(i)/(v_fluid(i)*...
227             rho_inside*Cp_inside)+T_fluid_2(i);
228     else % Turn of solar collector if eta<0
229         Q_flat(i)=0;
230         T_fluid_out_flat(i)=T_fluid_2(i);
231     end
232     Sum_energy_flat=sum(Q_flat);
233     Sum_energy_low_temp=sum(Q_tot_unglazed);
234     Sum_energy_low_temp_solar=sum(Q_tot_radiation_low);
235     Sum_energy_low_temp_cond=sum(Q_tot_condensation_low);
236     Sum_energy_low_temp_conv=sum(Q_tot_convection_low);
237 end
238
239 Sum_energy_total_kwh=Sum_energy_low_temp/1000;
240 Sum_energy_radiation_kwh=Sum_energy_low_temp_solar/1000;
241 Sum_energy_conv_kwh=Sum_energy_low_temp_conv/1000;
242 Sum_energy_cond_kwh=Sum_energy_low_temp_cond/1000;
243 Sum_energy_flat_kwh=Sum_energy_flat/1000;
244
245 Hours_in_month=[1,744,1416,2160,2880,3624,4344,5088,...
246     5832,6552,7296,8016,8760];
247
248 for j=1:12
249     Energy_low_temp_month(j)=sum(Q_tot_unglazed...
250         (Hours_in_month(j):Hours_in_month(j+1)));
251     Energy_low_temp_solar_month(j)=sum(Q_tot_radiation_low...
252         (Hours_in_month(j):Hours_in_month(j+1)));
253     Energy_low_temp_cond_month(j)=sum(Q_tot_condensation_low...
254         (Hours_in_month(j):Hours_in_month(j+1)));
255     Energy_low_temp_conv_month(j)=sum(Q_tot_convection_low...
256         (Hours_in_month(j):Hours_in_month(j+1)));
257     Energy_flat_month(j)=sum(Q_flat...
258         (Hours_in_month(j):Hours_in_month(j+1)));
259 end
260 %Delta T
261 DeltaT=T_fluide_out_collector'-T_fluid;
262
263 set(0,'DefaultAxesFontSize',28)
264 figure
265 plot(1:i,Q_tot_unglazed(1:i)/A_solar)
266 title('Total power-output')
267 xlabel('Hour')
268 ylabel('Power [W/m2]')
269 xlim([0,i])
270
271 figure
272 plot(1:i,Q_tot_radiation_low(1:i)/A_solar)
273 title('Power contribution from solar radiation')
274 xlabel('Hour')
275 ylabel('Power [W/m2]')
276 xlim([0,i])
277
278 figure
279 plot(1:i,Q_tot_condensation_low(1:i)/A_solar)
280 title('Power contribution from condensation')
281 xlabel('Hour')

```

```

282     ylabel('Power [W/m2]')
283     xlim([0,i])
284
285     figure
286     plot(1:i,Q_tot_convection_low(1:i)/A_solar)
287     title('Power contribution from convection')
288     xlabel('Hour')
289     ylabel('Power [W/m2]')
290     xlim([0,i])
291
292     figure
293     plot(1:i,DeltaT(1:i))
294     title('Temperature difference between inlet and outlet')
295     xlabel('Hour')
296     ylabel('Delta T [C]')
297     xlim([0,i])
298
299     xlswrite('Output',Q_tot_unglazed,'Output')
300
301     else %Mode 2
302         for j=1:Temp_end
303             for i = 1:length(T_a)
304                 if T_a(i)>0
305                     tick=1;
306                     while n+1>tick
307                         %Calculate wind speed in collectorplane
308                         W_coll(i)=wind(i)*0.68-0.5;
309                         if W_coll(i)<0
310                             W_coll(i)=0;
311                         end
312
313                         %Calculate h_convetion, Bengt Peres
314                         h_conv=2.8+3*W_coll(i);
315
316                         %Calcualte energy from condensation, Bengt Peres
317                         T_s=T_fluid(i);
318                         rho_air=f_air_density2(T_a(i),humidity(i),p); %[kg/m3]
319                         humidity_ratio=convert_humidity(p,T_a(i)+...
320                             273.15,humidity(i), 'relative humidity',...
321                             'specific humidity');
322                         v_air=rho_air*humidity_ratio ; %[kg/m3]
323                         v_sat=0.001*(4.85+0.347*T_s+0.00945*T_s^2+...
324                             0.000158*T_s^3+0.00000281*T_s^4);
325                         Cp_air=1.005*10^3; %(kJ/(kg K))
326                         rw=2260*10^3; %Energy for the phase change
327
328                         q_condensation=rw*(h_conv/(rho_air*Cp_air))*...
329                             (v_air-v_sat); %W/m2
330
331                         %Define if there will be condensation or not
332                         if q_condensation>0
333                             Q_cond(tick)=q_condensation*A_solar/n;
334                             T_condensation_air=convert_humidity (p, T_a(i)+...
335                                 273.15, humidity(i), 'relative humidity',...
336                                 'dew point')-273.15; %[C]
337                             T_s=T_condensation_air;
338                         else

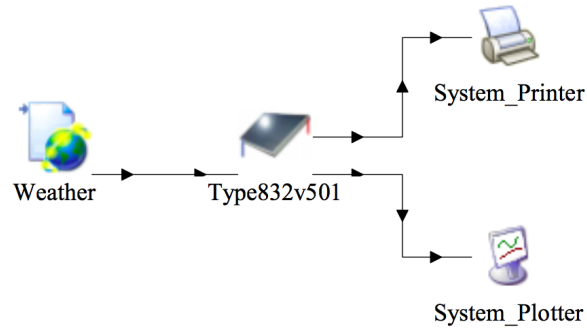
```

```
339         Q_cond(tick)=0;
340         T_s=T_fluid(i);
341     end
342
343     %-----
344     %Calculate h_inside, page 549
345     mu_inside=XSteam('my_pT',p_fluid,T_fluid(i));
346     if T_s>0
347         mu_surface=XSteam('my_pT',p_fluid,T_s);
348     else
349         mu_surface=mu_inside;
350     end
351
352     rho_inside=XSteam('rhoL_T',T_fluid(i));
353     Cp_inside=XSteam('CpL_T',T_fluid(i))*10^3; % [J/kgK]
354     k_inside=XSteam('tcL_T',T_fluid(i)); % [W/mK]
355     nu=mu_inside/rho_inside;
356     Re_D=(v_fluid(i)*Di)/(nu*A_inside);
357     Pr=mu_inside*Cp_inside/k_inside;
358
359     if Re_D>10000
360         Nu_D=0.027*Re_D^(4/5)*Pr^(1/3)*...
361             (mu_inside/mu_surface)^(0.14); %page 567
362     else
363         Nu_D=4.36; %Laminar, uniform q_s, page 567
364     end
365
366     h_inside=Nu_D*k_inside/Di; %page 549
367
368     %-----
369     %Calcualte energy from outdoor temperature diffrence
370     Q_conv(tick)=(T_a(i)-T_fluid(i))/((1/(h_conv*2*pi*...
371         L*(Do/2)))+(log((Do/2)/(Di/2))/(k_tube*2*pi*L))+...
372         (1/(h_inside*2*pi*L*(Di/2)))); %page 136
373
374     %-----
375     %Calcualte energy from Radiation, page 825
376     alpha_sky=epsilon_tube;
377     q_rad=alpha_tube*G(i)-(epsilon_tube*sigma*...
378         ((T_s+273.15)^4-(T_sky+273.15)^4));
379     Q_radiation(tick)=q_rad*A/2;
380
381     %Calculate total energy
382     Q_tot_low(tick)=Q_cond(tick)+Q_conv(tick)+...
383         Q_radiation(tick);
384
385     %Calculate temperature
386     T_fluid_out=Q_tot_low(tick)/(v_fluid(i)*rho_inside*...
387         Cp_inside)+T_fluid(i);
388     T_fluid(i)=T_fluid_out;
389
390     tick=tick+1;
391 end
392
393 %Sum energy
394 Q_tot_unglazed(i)=sum(Q_tot_low);
395 Q_tot_radiation_low(i)=sum(Q_radiation);
```

```
396         Q_tot_condensation_low(i)=sum(Q_cond);
397         Q_tot_convection_low(i)=sum(Q_conv);
398
399         if Q_tot_unglazed(i)>0
400             Q_tot_unglazed(i)=Q_tot_unglazed(i);
401             Q_tot_radiation_low(i)=Q_tot_radiation_low(i);
402             Q_tot_condensation_low(i)=Q_tot_condensation_low(i);
403             Q_tot_convection_low(i)=Q_tot_convection_low(i);
404             T_fluide_out_collector(i)=T_fluid_out;
405         else % Turn of solar collector if Q>0
406             Q_tot_unglazed(i)=0;
407             Q_tot_radiation_low(i)=0;
408             Q_tot_condensation_low(i)=0;
409             Q_tot_convection_low(i)=0;
410             T_fluide_out_collector(i)=T_fluid_2(i);
411         end
412     else
413         Q_tot_unglazed(i)=0;
414         Q_tot_radiation_low(i)=0;
415         Q_tot_condensation_low(i)=0;
416         Q_tot_convection_low(i)=0;
417         T_fluide_out_collector(i)=T_fluid_2(i);
418     end
419     T_fluid(i)=T_fluid_2(i); %Reset fluid-temperature
420
421     %Calculate Rho and cp for the fluid inside solar collector
422     rho_inside=XSteam('rhoL_T',T_fluid_2(i));
423     Cp_inside=XSteam('CpL_T',T_fluid_2(i))*10^3; % [J/kgK]
424
425     %-----
426     %Flat plate solar collector, see "Solvarme i bostader med
427     %analys av kombinationen solfangare och bergvarmepump"
428     %-----
429     eta_flat= (G(i)*n0-a1*(T_fluid_2(i)-T_a(i))-a2*...
430         ((T_fluid_2(i)-T_a(i))^2))/G(i);
431     if 1000>eta_flat && eta_flat>0 && eta_flat~=-inf
432         Q_flat(i)=eta_flat*G(i)*A_solar;
433         T_fluid_out_flat(i)=Q_flat(i)/(v_fluid(i)*rho_inside*...
434             Cp_inside)+T_fluid_2(i);
435     else % Turn of solar collector if eta<0
436         Q_flat(i)=0;
437         T_fluid_out_flat(i)=T_fluid_2(i);
438     end
439     Sum_energy_flat=sum(Q_flat);
440     Sum_energy_low_temp=sum(Q_tot_unglazed);
441     Sum_energy_low_temp_solar=sum(Q_tot_radiation_low);
442     Sum_energy_low_temp_cond=sum(Q_tot_condensation_low);
443     Sum_energy_low_temp_conv=sum(Q_tot_convection_low);
444 end
445     Sum_energy_total_kwh(j)=Sum_energy_low_temp/1000;
446     Sum_energy_radiation_kwh(j)=Sum_energy_low_temp_solar/1000;
447     Sum_energy_conv_kwh(j)=Sum_energy_low_temp_conv/1000;
448     Sum_energy_cond_kwh(j)=Sum_energy_low_temp_cond/1000;
449     Sum_energy_flat_kwh(j)=Sum_energy_flat/1000;
450
451     T_fluid=T_fluid+1;
452     T_fluid_2=T_fluid_2+1;
```

```
453     end
454
455     x_varde=Temp_start:Temp_end;
456     set(0,'DefaultAxesFontSize',28)
457     plot(x_varde,Sum_energy_total_kwh/A_solar)
458     hold on
459     plot(x_varde,Sum_energy_flat_kwh/A_solar,'--')
460     plot(x_varde,Sum_energy_radiation_kwh/A_solar)
461     plot(x_varde,Sum_energy_conv_kwh/A_solar)
462     plot(x_varde,Sum_energy_cond_kwh/A_solar)
463     legend('Total energy gain (Low temp. solar collector)',...
464           'Total energy gain (Glazed flat plate collector)',...
465           'Energy from solar radiation included radiation losses',...
466           'Energy from convection', 'Energy from condensation')
467     xlabel('Fluid temperature [C]')
468     ylabel('Energy per year [kWh/m2]')
469 end
```


Appendix B TRNSYS

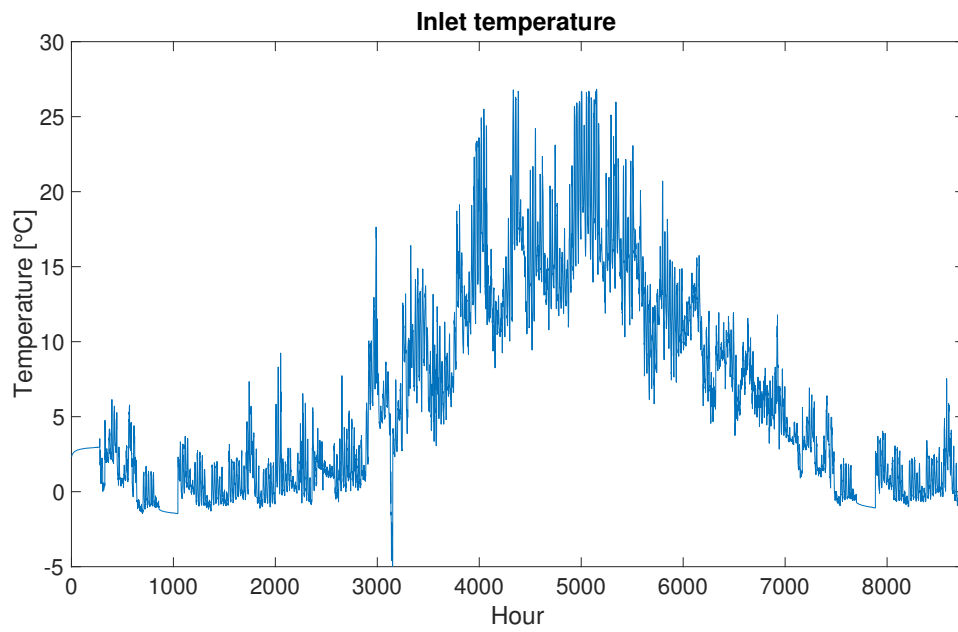


TRNSYS-model of low-temperature solar collector.

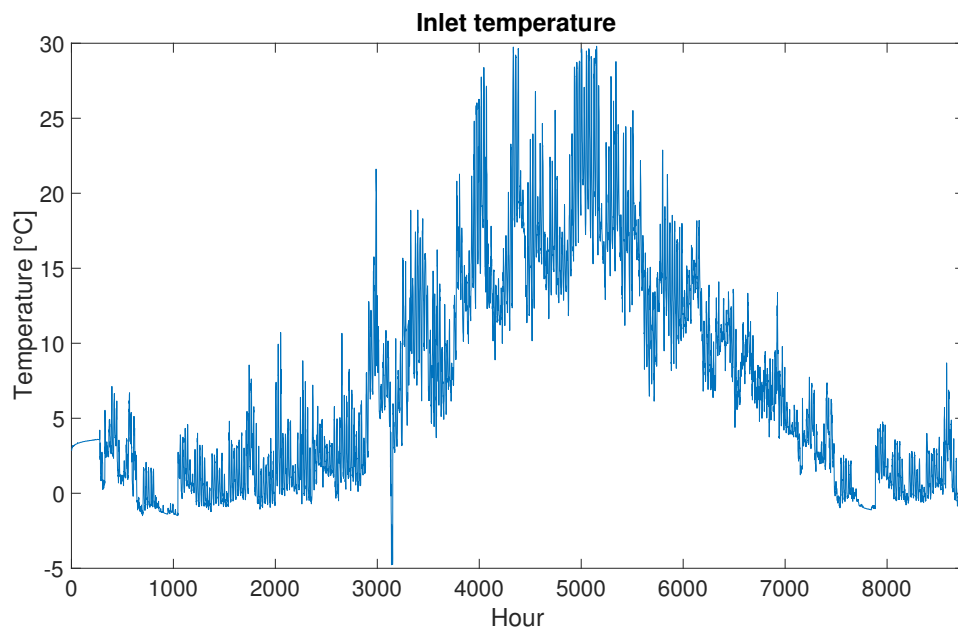
Parameters, Type832v501

Eta0 - Optical efficiency	0.9
Kdiff - IAM for diffuse radiation	0.9
a1 - Linear heat loss coefficient	8 [W/m ² K]
a2 - Quadratic heat loss coefficient	0.007 [W/m ² K ²]
cwhl - Wind speed dependency of heat losses	6.25
cIR - Infrared radiation dependency of collector	0.14
wf - Wind speed factor	0.5
rf - Sky radiation factor	1
ccond - Coefficient for condensation gains	0.917

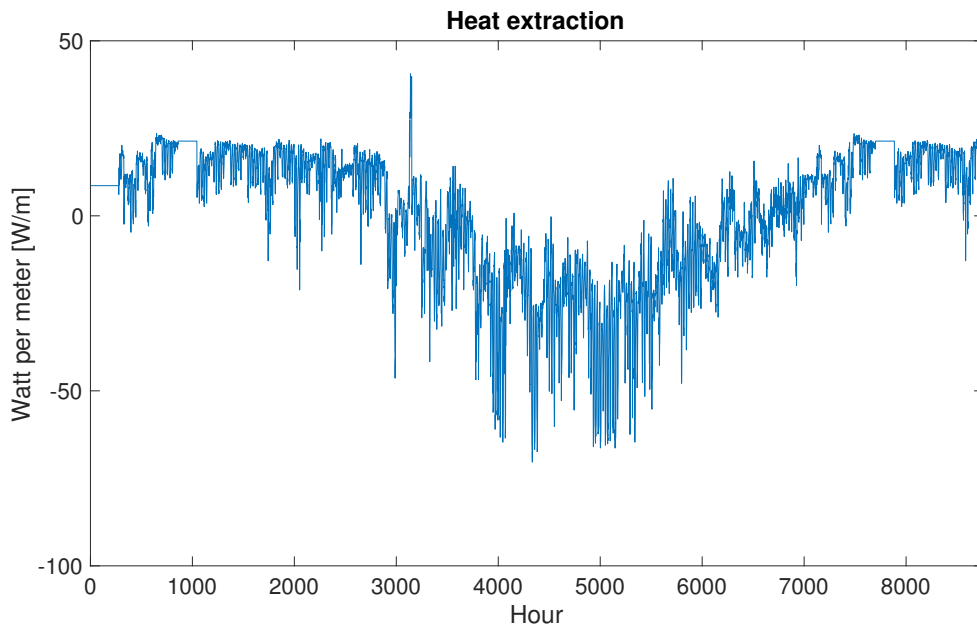
Appendix C EED



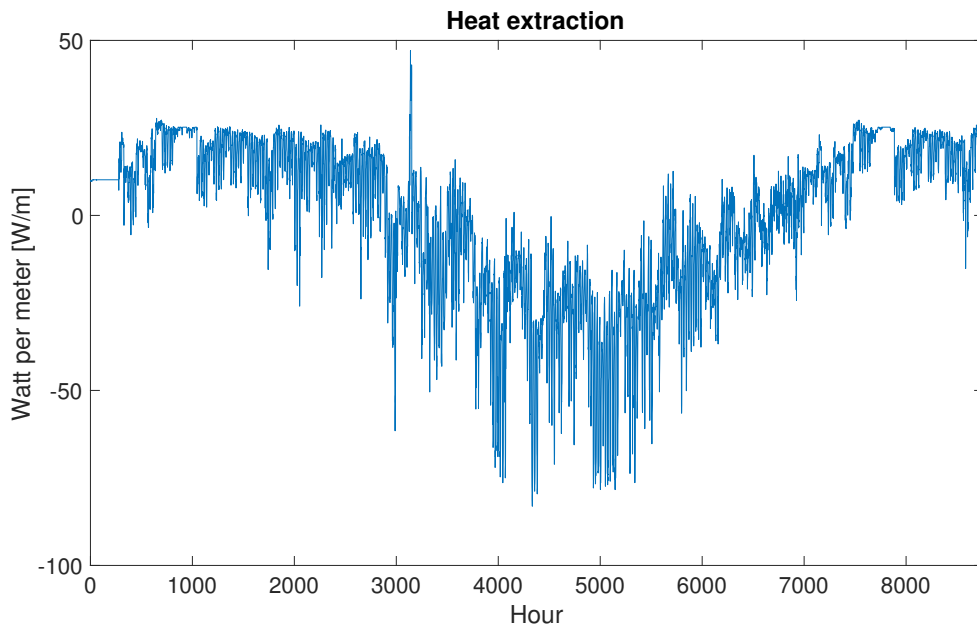
Temperature before BTES without solar collector.



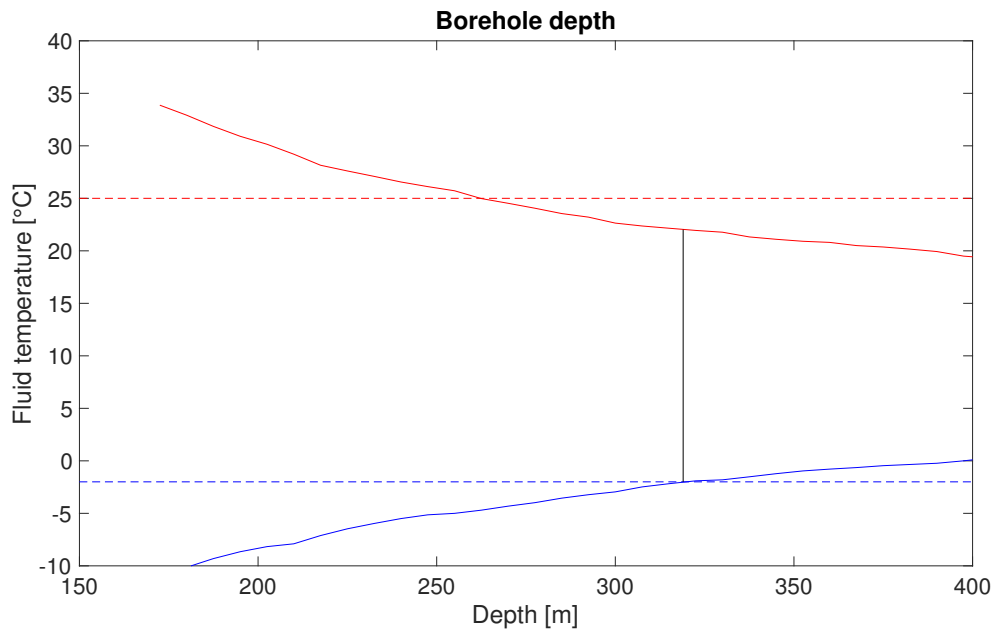
Temperature before BTES with 360 m² solar collector.



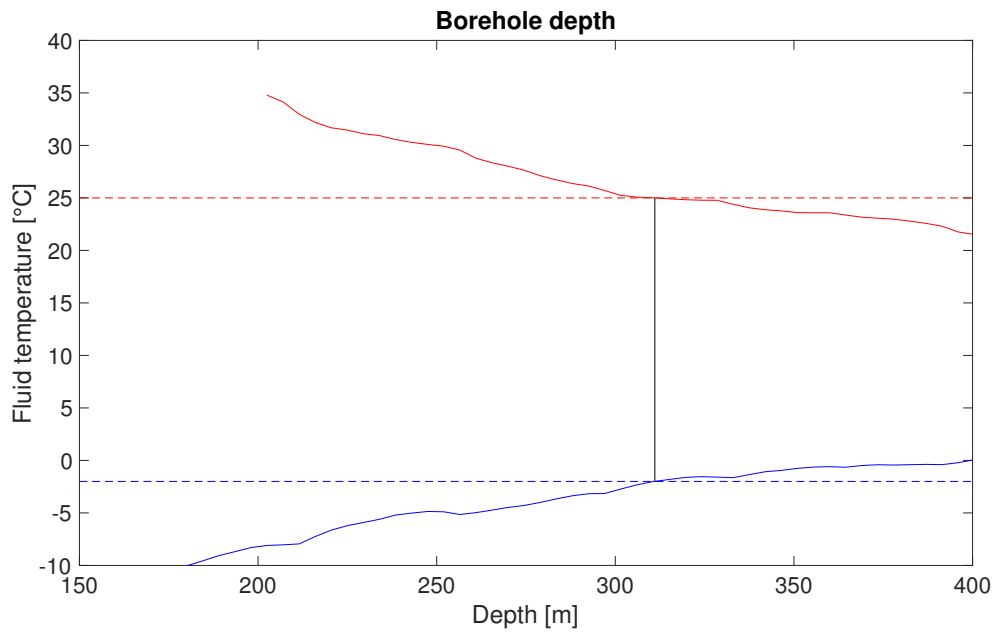
Heat extraction without solar collector.



Heat extraction with 360 m² solar collector.



Borehole depth without solar collector.



Borehole depth with 360 m² solar collector.

Master's Thesis BOMX02-18-2
Department of Architecture and Civil Engineering
Division of Building Services Engineering
Chalmers University of Technology
SE-412 96 Gothenburg
Sweden